Late Caledonian transpression and the structural controls on pluton construction; new insights from the Omey Pluton, western Ireland

William McCarthy[1*], R. John Reavy[2], Carl T. Stevenson[3] and Michael S. Petronis[4]

[1] Department of Earth & Environmental Sciences, University of St Andrews, St Andrews, Fife, KY16 9AL, UK. Email: wm37@st-andrews.ac.uk
[2] School of Biological, Earth and Environmental Sciences, University College Cork, Cork, Ireland.
[3] School of Geography, Earth and Environmental Sciences, University of Birmingham, Birmingham B15 2TT, UK.
[4] Environmental Geology, Natural Resource Management Department, New Mexico Highlands University, Las Vegas NM 87701, USA.
*Corresponding author

ABSTRACT: The Galway Granite Complex is unique among the British and Irish Caledonian granitoid terranes, as it records punctuated phases of magmatism from ~425–380 Ma throughout the latest phase of the Caledonian Orogeny. Remapping of the Omey Pluton, the oldest member of this suite, has constrained the spatial distribution and contact relationships of the pluton's three main facies relative to the nature of the host rock structure. The external contacts of the pluton are mostly concordant to the limbs and hinge of the Connemara Antiform. New AMS data show that a subtle concentric outward dipping foliation is present, and this is interpreted to reflect pluton inflation during continued magma ingress. Combined field, petrographic and AMS data show that two sets of shear zones (NNW–SSE and ENE–WSW) cross-cut the concentric foliation, and that these structures were active during the construction of the pluton. We show that regional sinistral transpression at ~420 Ma would have caused dilation along the intersection of these two fault sets, and suggest that this facilitated centralised magma ascent. Lateral emplacement was controlled by the symmetry of the Connemara Antiform to ultimately produce a discordant phacolith. We propose that regional sinistral transpression at ~420 Ma influenced the siting of smaller intrusions over NNW–SSE faults, and that the later onset of regional transtension caused larger volumes of magma to intrude along the E–W Skird Rocks Fault at ~400 Ma.

KEY WORDS: Anisotropy of magnetic susceptibility, anticline, ascent and emplacement, Caledonian granite, flow, fold, Galway Granite Complex, microstructure, phacolith, transpression

The study of granitoid complexes allows temporal and kinematic constraints to be assigned to orogenic processes (Hutton 1988, Pitcher 1998). A compilation of publications on individual plutons in Britain and Ireland have enabled orogenic scale models to be developed for this sector of the Caledonian Orogen (e.g., Stone *et al.* 1997; Brown *et al.* 2008; Neilson *et al*. 2009). The Silurian–Devonian Galway granites in western Ireland are unique, as they were emplaced over a protracted period between ~425 Ma and 380 Ma at a critical stage in Palaeozoic tectonics (Feely *et al.* 2010). Collectively, these data highlight temporal discrepancies in recent regional petrogenetic models, that require the cessation of magmatism north of the Orlock Bridge Fault by 410 Ma (Brown *et al.* 2008), because they show that Caledonian magmatism occurred both before and after 410 Ma north of the Orlock Bridge Fault. The longevity of magmatism in Connemara thus presents a unique opportunity to study the chemical, structural and kinematic evolution of the latter part of the Caledonian Orogeny.

Preliminary mapping by the Geological Survey of Ireland shows that the Silurian–Devonian Galway Granites (Fig. 1) includes the Main Batholith and several spatially distinct smaller plutons (Kinahan 1869, 1878). Extensive chronological and field-based research demonstrates the Main Batholith intruded into an E–W extensional structure, i.e., the Skird Rocks Fault, at ~400 Ma during regional sinistral transtension (Leake 1974, 2008; Max *et al.* 1978; Madden 1987; Ryan *et al.* 1995; Desouky *et al.* 1996; Feely *et al.* 2003; Baxter *et al.* 2005). The structural relationship between the surrounding intrusions and the Main Batholith is not yet established; however, recent work has shown that one of these, the Roundstone Pluton, intruded at ~420 Ma (U–Pb LA–ICP–MS (McCarthy 2013)) and that magma ascent was structurally controlled by a reactivated subvertical NNW–SSE fault (McCarthy *et al.* 2015). This work infers that individual plutons ascended along faults of different orientations and that this may have been determined by the kinematic switch between regional transpression and transtension at the end of the Caledonian Orogeny (Dewey & Strachan 2003). Molybdenite Re–Os geochronology data show the Omey Pluton is ~422.5 ± 1.7 Ma (Feely *et al.* 2007), and most likely predates all other intrusions associated with this complex. Despite the profound temporal significance of the Omey Pluton, there is a dearth of information regarding the geology of this intrusion. Consequently, the structural relationship between it and other plutons is unknown and its significance within the context of regional petrogenetic models remains enigmatic.

 doi:10.1017/S1755691015000201

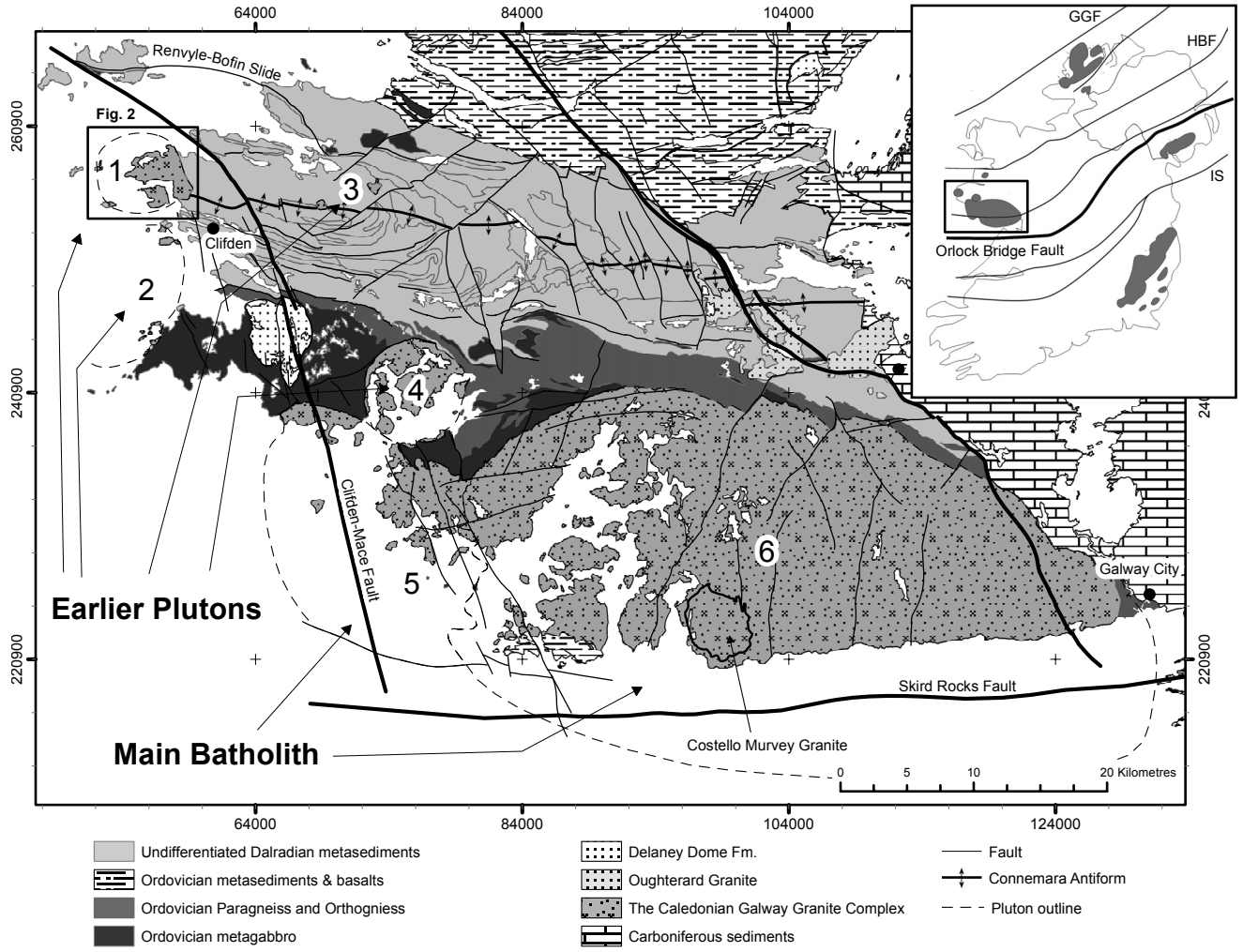

Figure 1 Summarised geology of the Connemara Metamorphic Complex and the late Caledonian Galway Granite Complex (GGC). The GGC constitutes the Earlier Granites (the Omey Pluton (1); the Inish Pluton (2); the Letterfrack Pluton (3); and the Roundstone Pluton (4)) and the Main Batholith (a composite of the Carna Pluton (5) and the Kilkieran Pluton (6)). The axis of the D4 Connemara Antiform trends ESE–WNW and is cross-cut by the Omey Pluton in the west. Several NW–SE and SW–NE D5 faults cross the GGC.

In this contribution, we clarify the nomenclature pertaining to the Siluro-Devonian granitoids in Galway. New field data describe the petrological facies, facies distribution and geometry of the Omey Pluton and constrain its stratigraphic position within the folded Dalradian host rock. New anisotropy of magnetic susceptibility (AMS) data and field data show that a subtle concentric pluton inflation fabric is cross-cut by a suite of NNW–SSE and E–W faults, and that these faults were active as ductile shear zones during pluton construction. We show that while the shape of the intrusion was dictated by the structure of the folded host rock, fabrics recorded within the pluton reflect inflation and concurrent shearing along NNW–SSE and E–W faults that cross-cut the pluton. Based on these observations, we propose that centralised magma ascent was achieved along the intersection of these deep-seated subvertical faults that were reactivated as magma conduits due to ambient regional transpression.

1. Geological background

1.1. The Connemara Metamorphic Complex

The bedrock geology of Connemara consists of a fold and thrust sequence, known as the Connemara Metamorphic Complex (CMC) (Leake & Tanner 1994), which is intruded by a series of Siluro-Devonian granitoids (Fig. 1). The hanging wall of the CMC consists of Dalradian strata that are cross-cut and metamorphosed by Ordovician orthogneiss and metagabbros associated with the Grampian Orogeny (Friedrich *et al.* 1999a, b). This sequence of rocks was thrust southwards over the Delaney Dome Formation along the Mannin Thrust during the closure of the Iapetus Ocean (Leake *et al.* 1983; Leake 1986; Tanner *et al.* 1989). The CMC underwent five phases of deformation (D1–D5) before initiation of late Caledonian magmatism (Leake & Tanner 1994); D4 and D5 being of most significance to the current work. Strain imparted during D4 formed the regional scale Connemara Antiform, a gently ESE-plunging fold across central Connemara. D5 formed N–S-trending open folds and is associated with substantial shearing along large NNW–SSE and NNE–SSW conjugate faults. Here, reactivation of D5 faults during the Silurian is associated with concurrent regional sinistral strike slip (Leake & Tanner 1994).

1.2. The Galway Granite complex defined

The Siluro-Devonian Galway granites, often referred to as the late Caledonian Galway Granites (Graham *et al.* 2000; Suzuki *et al.* 2001; Selby *et al.* 2004), refer to a suite of granitoids that were emplaced into the CMC between 425 Ma and 380 Ma (Feely *et al.* 2010). These include the 'Main Batholith' and associated 'Satellite Plutons'; i.e., the Omey, Inish, Letterfrack and Roundstone plutons (Fig. 1). The 'Main Batholith' is composed of two distinctive parts. An oval shaped NNW–SSE

https://doi.org/10.1017/S1755691015000201 Published online by Cambridge University Press

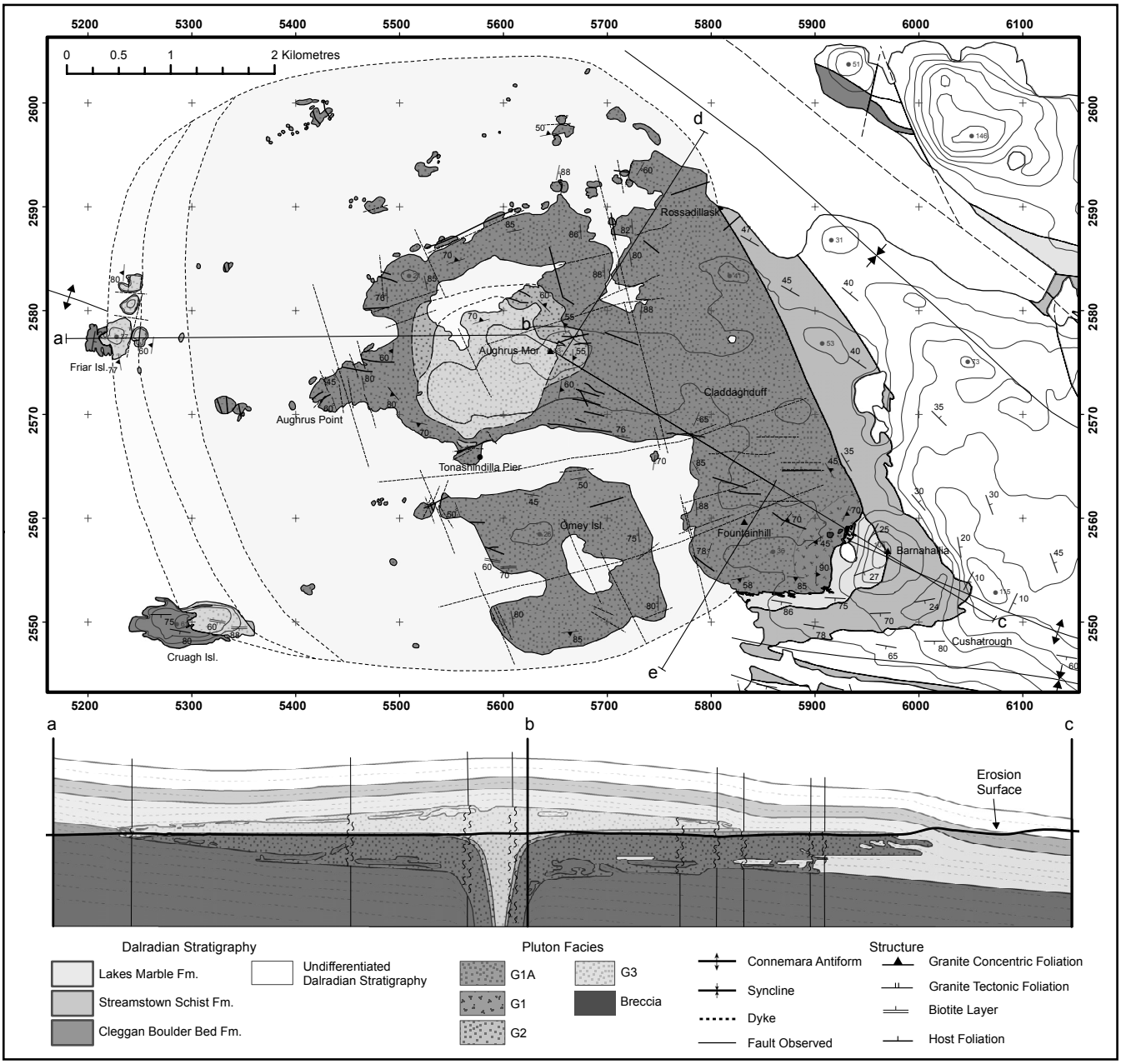

Figure 2 Geological map of the Omey Pluton showing facies distribution, internal structure and host rock structure, which is dominated by the D4 Connemara Anticline. Observed intrusive contacts are largely concordant and the intrusion is cross-cut by a series of NNW–SSE and E–W shear zones. Schematic cross-section of the Omey Pluton depicts lateral emplacement of magma along the axis of the Connemara Antiform.

oriented intrusive body, recently described as the "Western Ring Complex of the Galway Granite Batholith" (Leake 2011), forms the western portion of the Main Batholith (Fig. 1(5)). Molybdenum Re–Os geochronology shows this part of the pluton to be ~410 Ma (Selby *et al.* 2004). To the east, a larger (~1200 km^2), younger, ESE–WNW orientated oval intrusion forms the larger portion of the Main Batholith (Fig. 1(6)). Zircon U–Pb geochronology shows this part of the pluton to be ~400 Ma (Feely *et al.* 2003). The observations of Max *et al.* (1978), Wright (1964) and Leake (2011) also report compositional and structural differences between the east and west parts of the Main Batholith. Therefore, the 'Main Batholith' is here defined as a composite batholith of two discrete parts; the earlier 'Carna Pluton' in the west (Fig. 1(5)) and the adjoining 'Kilkieran Pluton' to the east (Fig. 1(6)).

A misleading phrase used in reference to the Galway Granites is 'Satellite Plutons'. The prefix 'satellite' implies that these plutons intruded around, and were inherently satellites to, the Main Batholith. This is not the case, as the Main Batholith is ~410–380 Ma (Feely *et al.* 2003, 2010) and the 'Satellite' plutons are understood to be ~425–420 Ma (Elias *et al.* 1988; Buchwaldt *et al.* 2001; Feely *et al.* 2007). Therefore, the use of the term 'satellite' is incorrect and unnecessarily confusing. We propose that the Inish, Letterfrack, Omey and Roundstone plutons should be referred to collectively as the 'Earlier Plutons' as this term accurately depicts these as standalone plutonic bodies that predate the Main Batholith. Magmatism in the Galway Granite Complex (GGC) initiated during Caledonian regional transpression (Dewey & Strachan 2003; Soper & Woodcock 2003) and terminated 10 Ma after the Acadian Orogeny (Meere & Mulchrone 2006; Woodcock *et al.* 2007). Therefore, magma was generated and emplaced concurrently with two major orogenic events over a period of at least 40 Ma. Thus, we suggest that the suite of Silurian–Devonian

https://doi.org/10.1017/S1755691015000201 Published online by Cambridge University Press

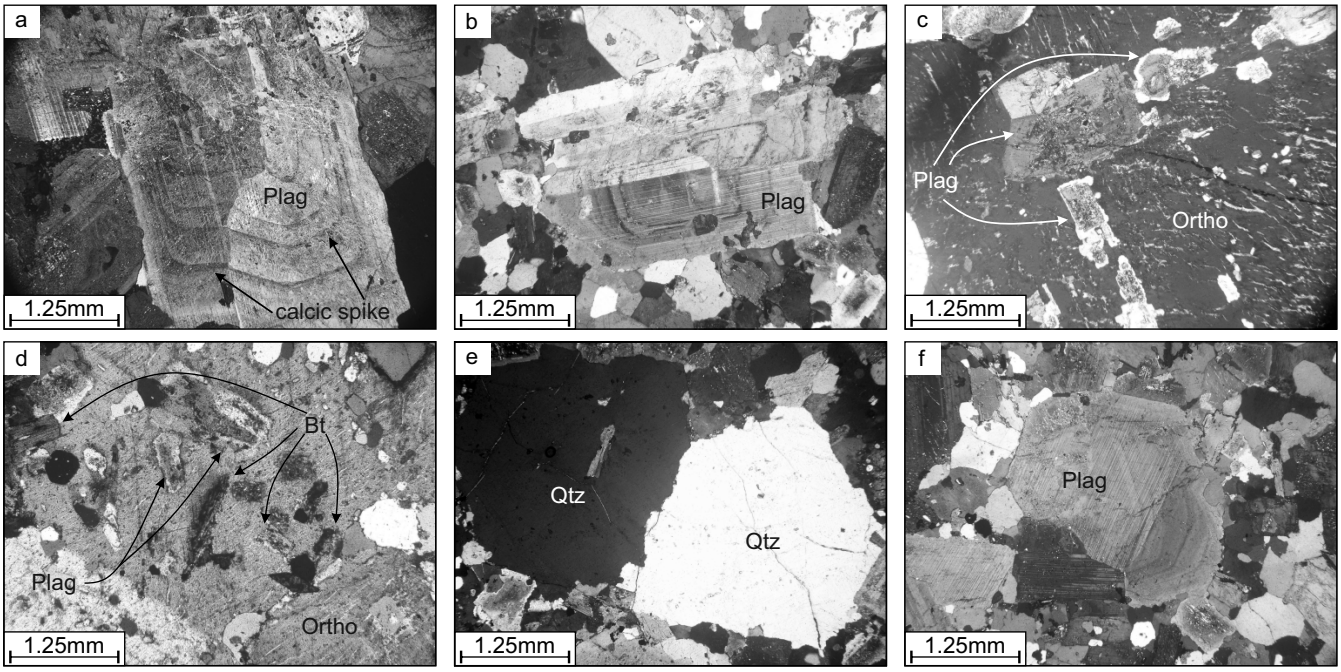

Figure 3 Characteristic petrographic features of facies G1 and G2. Seriticised calcic spikes within plagioclase (Plag) (a, b) and poikilitic K-feldspar (Ortho) crystals which exhibit inclusions of 0.5–2-mm quartz (Qtz), euhedral feldspar and oxides which accreted to, or nucleated on, the former outer margins of the phenocryst (c, d). G2 is distinguished from G1 by the presence of larger K-feldspars (c) and rounded quartz and plagioclase phenocrysts (e, f).

granites in Connemara, be referred to as the 'Galway Granite Complex', as the current data set suggest it is not all of Caledonian origin.

2. Field observations and petrography

All grid references refer to Irish National Grid (GCS_TM65). The Omey Pluton (Fig. 2) is approximately circular, has a surface area of ~175 km^2 and was emplaced into the Argyll Group of the Dalradian Supergroup, within the hinge of the Connemara Antiform (Cobbing 1969). Originally described as a "normally zoned forcefully emplaced granite with a central acidic plug derived from the concentration of volatiles during cooling" (Townend 1966), petrographic and geochemical studies indicate that this intrusion is epizonal, having been emplaced between 2.5 and 3.3 kbar (Ferguson & Harvey 1979; Ferguson & Al-Ameen 1986; Ahmed-Said & Leake 1996). Fluid inclusion analysis of vein-hosted and disseminated molybdenite within the granite suggests mineralisation immediately followed crystallisation at 422.5 $\pm$ 1.7 Ma (molybdenite Re–Os age determination), and therefore provides a minimum age of crystallisation (Feely *et al.* 2007).

2.1. Facies definition

Following Townend (1966), detailed remapping of the intrusion (Fig. 2) has resulted in considerable modifications in terms of facies definition, distribution and contact relationships. The Omey Pluton is a composite intrusion consisting of three main facies, G1, G2 and G3, previously termed the Omey Adamellite, the Aughrus More Adamellite and the Island Adamellite respectively (Townend 1966). The Glassillaun Granodiorite, previously described as a sub-facies of G1 (Townend 1966), is now recognised as a series of E–W-striking porphyritic microgranite dykes hosted within G1 and not a distinct facies of the pluton (Fig. 2). Townend (1966) also described the petrology and nature of lamprophyre and hornblende plagioclase porphyritic dykes which occur throughout the pluton, trending NNW–SSE or WSW–ENE and cross-cutting the granite and which, therefore, are <422 Ma.

Omey Island and a large proportion of the Aughrus Peninsula are composed of the G1 facies which makes up ~75 % of the surface area of the pluton (Fig. 2). An array of small rocky sea stumps and islands lie 100–1000 m offshore to the W and N; the majority of these are also composed of G1. In the east, near Barnahallia Lough, G1A is defined by a notable increase in the abundance of 3-mm prismatic dark green hornblende (2 %). South of Aughrusbeg Lough ([055770, 258230]) and north of Tonashindilla Pier ([055790, 256650]), a circular body of G3 (diameter ~1.2 km) forms the core of the Aughrus Peninsula and the highest point within the pluton, Aughrus More (146 m, [056475, 257626]). In the west, Cruagh Island and Friar Island are composed predominantly of G3. G2 is only found between G1 and G3. The largest exposures of G2 skirt around the NW and NE perimeter of the large exposure of G3 in the centre of the Aughrus Peninsula. The G2 facies is also present on the eastern tip of both Friar Island and Cruagh Island, and immediately north of Tonashindilla Pier (Fig. 2).

G1 is a medium-grained (8-mm) equigranular biotite hornblende monzogranite with rare 2 cm-long tabular phenocrysts of zoned plagioclase with seriticised calcic spikes (Fig. 3a, b). Rock mode is 30 % alkali feldspar, 34 % oligoclase-andesine, 30 % quartz, 3 % biotite, >2 % hornblende and 1 % accessories. Overall, this facies contains 72 SiO_2 wt.% (Leggo *et al.* 1966). Typically, subhedral K-feldspar occurs as 10-mm crystals amongst slightly finer-grained quartz and biotite. Prismatic titanite and zircon, along with apatite and rutile, are common accessory minerals.

G2 is a medium-grained biotite hornblende monzogranite and is very similar to G1, having a mode of 29 % alkali feldspar, 33 % andesine, 34 % quartz, 3 % biotite and 1 % accessories. G2 is finer grained (~6 mm), contains a lower abundance of hornblende (0–1 %) and exhibits very rare large phenocrysts of tabular K-feldspar up to 4 cm long. K-feldspar phenocrysts

https://doi.org/10.1017/S1755691015000201 Published online by Cambridge University Press

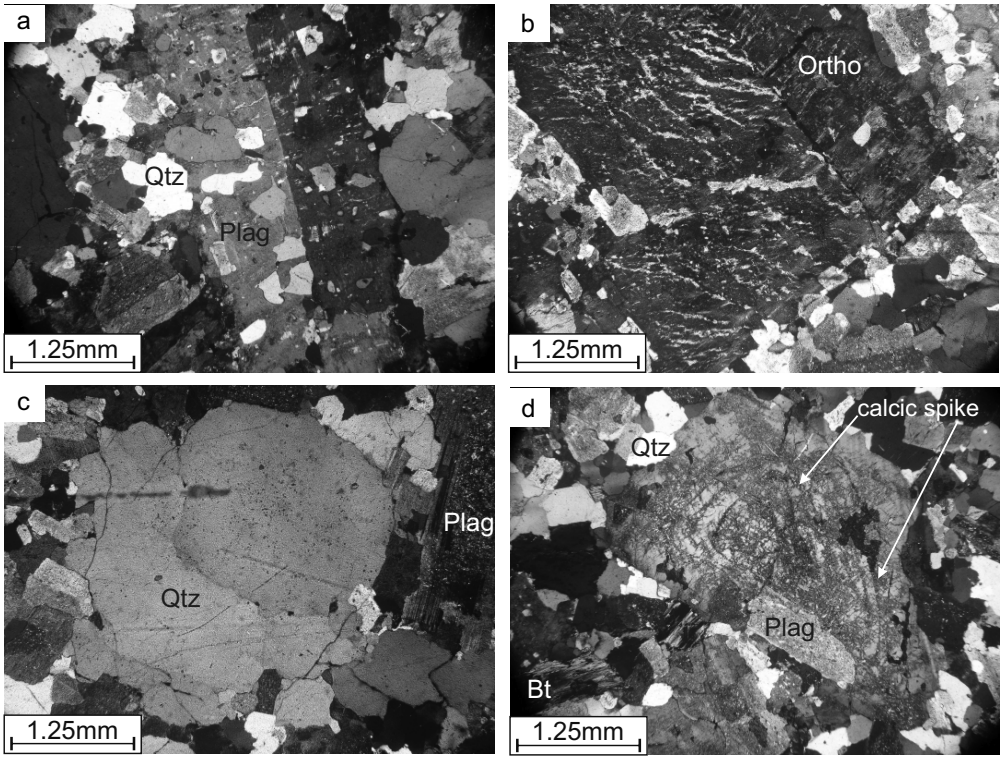

Figure 4 Characteristic petrographic features of G3. Porphyritic texture defined by ≤15-mm tabular plagioclase (Plag) and perthitic orthoclase (Ortho) (a, b) and ≤12-mm studs of anhedral or rounded quartz (Qtz) (c). Seriticised plagioclase is concentrated along calcic rich cores and calcic zones (d).

exhibit inclusions of quartz, biotite and plagioclase which are arranged and aligned in concentric zones within the crystal and against its faces via synneusis (Fig. 3c, d) (Vance 1969). Quartz and feldspar commonly occur as rounded 6–8-mm grains (Fig. 3e, f), or as slightly elongate lobes which, with biotite, define subtle foliations when fabrics are present.

G3 is a medium- to fine-grained (~2–6 mm) pink quartz-phyric monzogranite (Fig. 4). Accessory minerals include zircon, apatite, rutile and fluorite. Rock mode is 30 % K-feldspar, 32 % oligoclase, 35 % quartz, 2 % biotite, >1 % muscovite and >1 % accessories. Biotite is far less abundant, muscovite is present but rare and hornblende is absent; oligoclase is the dominant feldspar. Magnetite is present in lower abundances than those observed in earlier facies and a higher proportion of hematite is present (see online Appendix – Supplementary Magnetic Data). This facies has a slightly higher SiO_2 content (75 SiO_2 wt.% (Leggo *et al.* 1966)) and fewer mafic minerals than G1 and G2, and is interpreted to represent a more evolved magma. The G3 facies characteristically exhibits a porphyritic texture defined by ≤15-mm tabular plagioclase and orthoclase (Fig. 4a, b) and ≤12-mm studs of anhedral or rounded quartz (Fig. 4c) set in a 2–5-mm monzogranite groundmass. Quartz phenocrysts exhibit minor undulose extinction and are approximately spherical. Fluorite associated with biotite layering on Cruagh Island is associated with a concentration of late-stage residual fluids rich in incompatible elements near the upper portions of the intrusion (Townend 1966).

All facies plot towards the lower right of the monzogranite field, with a general trend from G1 to G3 becoming more quartz rich and less mafic. G1 and G2 are texturally and petrographically quite similar and are best distinguished by the presence of larger K-feldspars (Fig. 3c, d) and rounded quartz in G2 (Fig. 3e), and by a higher abundance of hornblende in G1. In both cases, prismatic green hornblende (~2–4 mm) is typically fresh, while biotite (2–6 mm) is almost always euhedral (outside of shear zones) and extensively chloritised. Plagioclase is partially altered and commonly extensively replaced by sericite (Fig. 3a). A broad variety of zoning textures are noted in both sodic and potassium-rich feldspars, including oscillatory, normal and rarely boxy zoning (Figs 3a, b, 4d). K-feldspar regularly exhibits a dramatic microperthite texture with thin exsolution lamellae of albite flames, which may be parallel or irregularly orientated (Fig. 3c). Although rare, the conversion of orthoclase to microcline is recorded and spatially associated with minor wedged twins in plagioclase, kinking and smearing of biotite. These features are associated with syn-post emplacement strain, a topic discussed further below.

2.2. External contact relationships

The external contacts of the pluton are best described relative to the axial trace of the D4 Connemara Antiform (Fig. 2). South of the axial trace, from Barnahallia southwest to Fountainhill Beach ([058293, 255265]) and on Cruagh Island, the granite is in contact with the steeply inclined (~80°) southward-dipping limb. North of the axial trace, from Barnahallia northwest to Rossadillask Beach ([058064, 259035]) the granite is in contact with the moderately inclined (~55°) northward-dipping limb of the antiform. Within the proximity of the fold hinge, at Barnahallia in the east and on Friar Island in the west, the granite is in contact with the gently eastward-plunging (~10°) axial trace.

Exposures of the western granite contact are limited to Cruagh Island and Friar Island (Fig. 2). On Cruagh Island, bedding dips steeply to the S (~75°) and strikes WNW–ESE; while on Friar Island, bedding dips 10–25° to the E and strikes NNE–SSW. Thus, Cruagh Island and Friar Island are the offshore representations of the southern limb and fold hinge of the Connemara Antiform respectively, although Friar Island probably sits slightly south of the actual fold hinge. Host rock strata is currently stratigraphically unassigned

https://doi.org/10.1017/S1755691015000201 Published online by Cambridge University Press

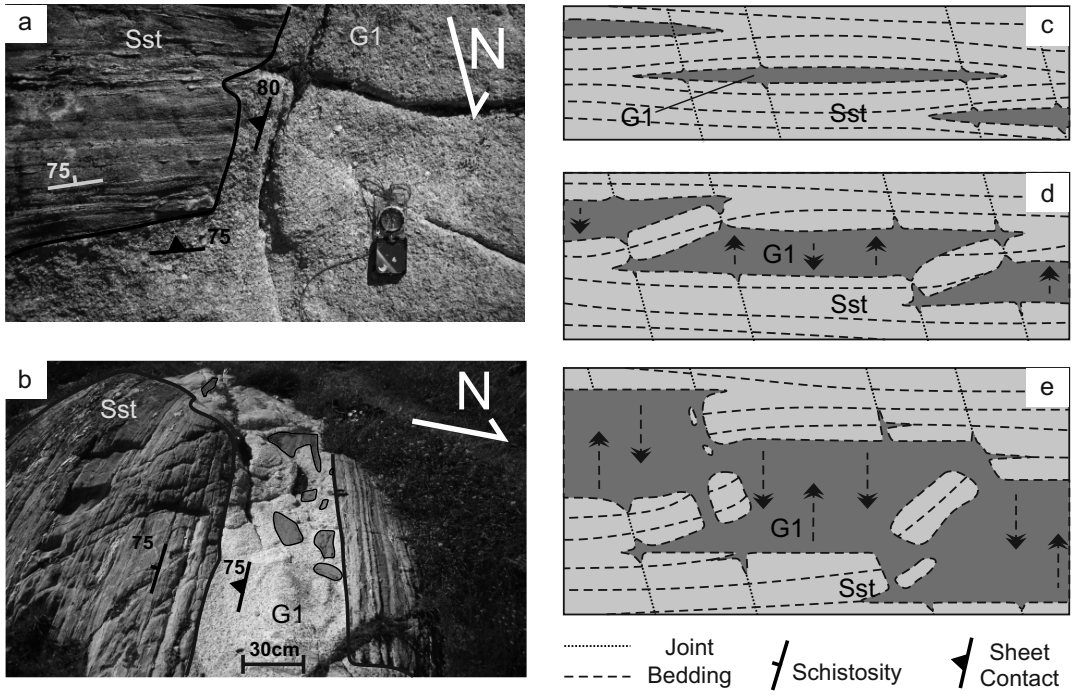

Figure 5 The southeastern pluton contact is, overall, concordant to the Dalradian country rock which dips steeply to the south (a, b). The folded stratigraphy is locally transgressed by sheets of magma which exploit joints and stope off small fragments of schist and psammite (c–e); these features are regarded as broken bridges (as defined by Hutton 2009).

(Leake & Tanner 1994; Long & McConnell 1995), and is dominated by well-bedded pelites and psammites. Townend (1966) described the presence of a narrow quartzite unit and several quartz pebble bed horizons on Cruagh Island; an observation supported here. Similarities between the quartz conglomerate units observed here and observations made by Kilburn *et al.* (1965) at Cleggan Head ([059600, 259900]), suggest that the stratigraphic units on these Islands can be correlated with the Cleggan Boulder Bed Formation.

2.2.1. Southern limb. The granite contact extends along an E–W trajectory from Fountain Hill Beach ([058260, 255260]) to Grallaghan ([059060, 255270]), before swinging north toward Barnahallia (Fig. 2). Here, the Streamstown Schist Formation (Badley 1976; Treloar 1977, 1982; Leake 1986; Leake & Tanner 1994) forms the bounding country rock.

Immediately south of Fountain Hill (Fig. 2), a well-defined steeply-dipping contact parallels the southward-dipping southern limb of the Connemara Antiform. Several intrusions of G1 and G1A extend from the pluton up to 50 m into the host rock, exploiting joints and compositional layering that ultimately define sheets which are largely concordant to the folded symmetry of the country rock (Fig. 5a, b). Abrupt undulations in the granite–country rock contacts in this area occur parallel to regional joint sets (NNW–SSE, WNW–ESE), and illustrate that localised discordant injection of magma was facilitated by pre-existing joint planes. These features are regarded as broken bridges (Hutton 2009; Schofield *et al.* 2012), where magma wedging preferentially exploits a vulnerable plane of weakness (bedding) and periodically sheets discordantly along a second pre-existing anisotropy (joints) (Fig. 5c–e).

Owing to better topographic relief and exposure, the sheeted nature of the granite contact is best observed in Cruagh Island. Situated on the southern limb of the Connemara Antiform, steeply-dipping (70–60° S) units of the Cleggan Boulder Bed Formation are intruded by concordant sheets of G3 which penetrate up to 50m into the country rock. Some large (1–5 m) detached blocks are present and local subtle chilled margins are observed.

2.2.2. Northern limb. The Lakes Marble Formation, which lies stratigraphically above the Streamstown Schist Formation (Badley 1976; Treloar 1977, 1982; Leake 1986; Leake & Tanner 1994), is in contact with the granite along the northern limb of the Connemara Antiform (Fig. 2). This contact relationship is best exposed on the eastern end of Rossadillask Beach ([058060, 259000]), where a sharp contact between the host rock and G1 parallels the northward-dipping limb of the Connemara Antiform. As observed further south, granite sheets extend up to 30 m into the host rock and are parallel to or discordantly cross-cut bedding along joint planes. A minor reduction in grain size over a few centimetres is occasionally accompanied by subtle contact-parallel foliations (Fig. 2).

2.2.3. Along the fold hinge. At the southeast granite contact, the axis of the Connemara Antiform is located just north of Barnahallia Lough. At this locality, the inclination of country rock bedding is slightly steeper than that observed further east along the fold hinge (10–20° *vs.* 5–10°). This implies that bedding has been vertically displaced at this locality, probably as a result of bifurcation of the host rock during inflation of granite sheets as magma intruded. At Barnahallia Lough, the Streamstown Schist Formation lies in direct contact with the Omey Pluton, while to the NW at [059240, 256450] the same can be said for the Lakes Marble Formation (Fig. 2). It is, therefore, clear that intruding granite cross-cuts the Streamstown Schist Formation at map scale (Fig. 2).

Due to abrupt topographic relief and good exposure, the attitude of the pluton's contact near the fold hinge of the Connemara Antiform is best observed on Friar Island (Fig. 6). The majority of the granite bedrock is G3; however, a small proportion of the eastern bedrock is part of the G2 facies (Fig. 2). The contact between G2 and G3 on Friar Island is gradational. An overall E–W reduction in grain size occurs toward the country rock contact, along with increasing numbers of small (usually cm-m scale) stoped blocks. A weak

https://doi.org/10.1017/S1755691015000201 Published online by Cambridge University Press

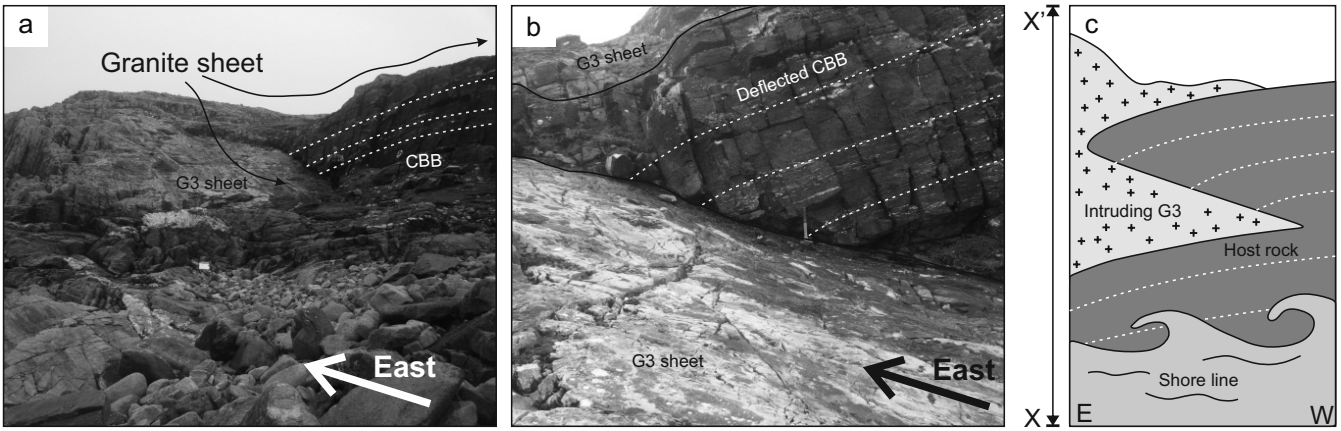

Figure 6 (a, b) Gently (10–20° E) eastward-inclined units of the Cleggan Boulder Bed Formation on Friar Island (see Fig. 2) show G3 intruded into and over the Cleggan Boulder Bed Formation, concordant to the primary schistosity and discordantly along inclined joint sets, along the fold axis of the Connemara Antiform. (c) A schematic section (looking south), depicting the perceived nature of the granite contact.

contact parallel foliation, steeply inclined to the west, is recorded. In the western extremity of the island, the Cleggan Boulder Bed Formation dips gently (~10°) to the east and strikes NNE–SSW. As observed at Barnahallia Lough in the east, the inclination of the country rock bedding increases slightly (~15–20°) eastwards toward the granite contact. At the contact, sheets of granite, some over 4 m thick, are plainly observed intruding into and above units of the Cleggan Boulder Bed Formation and along inclined joints (Fig. 6a, b). A schematic vertical profile looking south shows bedded schists, overlain by a thick granite sill, then a 3-m sequence of schists which is again overlain by a granite sheet (Fig. 6c). This suggests that vertical displacement of the gently inclined country rock was achieved in order to accommodate the lateral intrusion and thickening of granite sheets.

2.3. Internal contacts

Facies contacts are gradational, with the exception of some minor G3 sheets (~1 m) that cross-cut G2 to the NE of Aughrus More; these show that G3 post-dates G2. The G1–G3 contact can be observed toward the western end of the Aughrus Peninsula at [055193, 257203], where a gradational contact over 1 m dips gently toward the west (<5°). Critically, G3 lies on top of G1, suggesting that G3 was emplaced sub-horizontally over G1. A gradational contact over ~4 m is observed between G2 and G3 on Cruagh Island, Friar Island and near the summit of Aughrus More.

To the east and west of Aughrus More, mapped G1–G2 and G2–G3 contacts are approximately contour-parallel (Fig. 2), and so appear to be flat-lying. To the north and south of Aughrus More, mapped gradational contacts cross-cut topography and dip gently to the north and south, respectively. An ENE–WSW depression between Aughrus More and Aughrusbeg Lough reveal that G1–G2/G2–G3 contacts dip moderately to the west in this area.

2.4. Fabric development and sub-magmatic deformation

Characteristically weak, laterally discontinuous foliations defined by K-feldspar and euhedral platy biotite are observed sporadically within the pluton and define an overall concentric foliation (Fig. 2). This foliation is observed in G1 and G2, but not in G3. No systematic increase in fabric intensity is recorded in proximity to pluton margins. In thin section, quartz is typically anhedral and may exhibit weak undulose extinction. Chloritised biotite is euhedral, feldspars are idiomorphic and essentially unstrained, twinning in plagioclase is straight and only very rare examples of wedged twins are found. These features are characteristic of a dominantly magmatic or high-temperature weak sub-magmatic deformation, indicating that the observed fabrics formed prior to and during crystallisation (Vernon 2004; Passchier & Trouw 2005). These foliations are interpreted as pluton inflation fabrics which resulted from the continued injection of magma into the site of emplacement.

Townend (1966) identified two distinctive fault sets (NNW–SSE and E–W) which cross-cut all pluton facies (Fig. 2). Remapping has identified several prominent NNW–SSE and E–W topographic lows that cut through Aughrus More, Omey Island and define lakes, scarps and the shape of the coastline about the Omey Pluton (Fig. 2). E–W-trending faults are denoted by undulations in topography and sometimes weak fabric development. Porphyritic microgranite sheets which show variably unchilled and chilled margins intrude these structures (as do Carboniferous dolerite dykes and the lamprophyre dykes described by Townend (1966)).

NNW–SSE faults are more prominent and are denoted by minor intrusions and ~5 m-wide zones of moderate to strong sub-vertical NNW–SSE foliation (Fig. 7a). No consistent sense of shear has been identified along these faults. Marginal NNW–SSE sub-vertical foliations are defined by elongate quartz, aligned or smeared biotite and partially aligned feldspars, and intensify toward the centre of a shear zone. Brittle deformation occurs at the core of these structures and is expressed as intense, closely-spaced micro-fractures. In thin section, quartz ribbons are composed of multiple sub-grains which exhibit moderate undulose extinction, and biotite is variably kinked and smeared around euhedral feldspar phenocrysts (Fig. 7c). Feldspars incorporated into the foliation exhibit weak undulose extinction, orthoclase is sometimes partially converted to microcline and fractures are infilled with primary magmatic quartz (Fig. 7e, f). Such features are characteristic of sub-magmatic to solid-state deformation (Vernon 2004).

The field relationships and petrographic descriptions described show that the shear zones were established before the granite had cooled. These observations imply a concurrent relationship between shearing, which occurred mainly along NNW–SSE faults but also along E–W faults, and pluton construction.

3. Rock magnetic investigation

A total of 121 block samples were collected along an approximately evenly-spaced grid across the Omey Pluton, and

https://doi.org/10.1017/S1755691015000201 Published online by Cambridge University Press

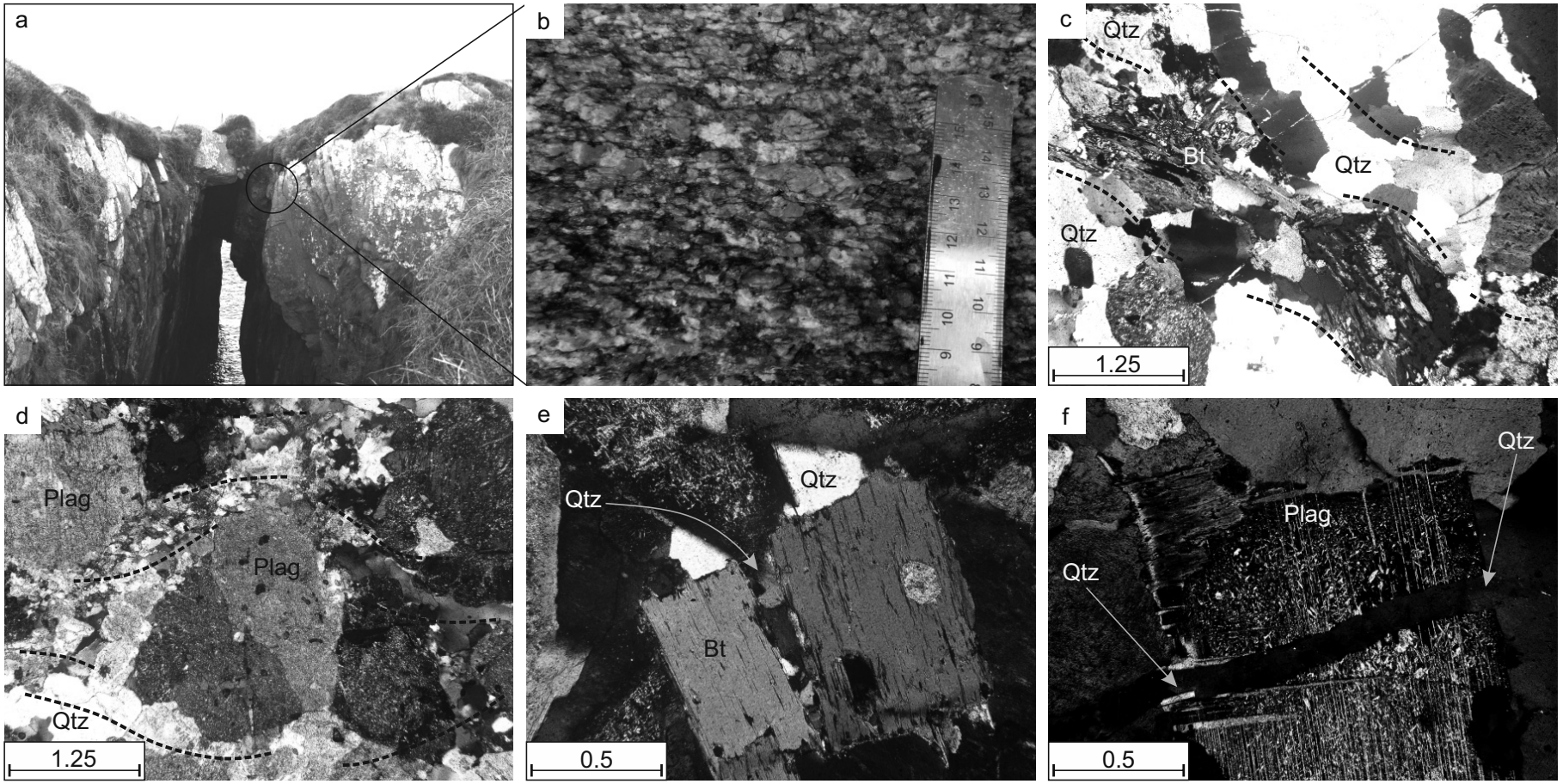

Figure 7 (a) A NNW–SSE shear zone from the northwestern portion of the Omey Pluton (see Fig. 2). (b) A moderate petrofabric within the shear zone parallels fine-scale micro fracturing, giving rise to a strong textural anisotropy. Petrographic observations show quartz ribbons (Qtz) and smeared biotite (Bt). (c) Marginal dynamic recrystallisation of plagioclase (Plag) along the foliation plane (d). Sub-magmatic deformation indicated by brittle fractures in biotite (e) and plagioclase (f), with primary quartz and biotite infill.

Table 1 Anisotropy of Magnetic Susceptibility data from the Omey Pluton, Western Ireland

Site ID	Facies	East	North	n	K3 Plunge	K3 Trend	K1 Plunge	K1 Trend	Km × 10^{-3}(SI)	H (%)	Pj	Tj
OM1	G1	057842	256311	11	44	69	34	299	11.32	4.11	1.02	0.06
OM1A	G1	057842	256311	9	48	60	35	279	11.21	2.7	1.017	0.42
OM2	G1	057817	256045	18	39	254	17	358	12.90	4.7	1.031	0.48
OM3	G1	059309	256393	13	22	244	68	61	11.01	4.7	1.039	0.95
OM4	G1	059224	256423	18	56	242	10	347	14.42	4.8	1.037	0.82
OM5	G1	058772	256267	21	22	251	63	109	14.77	6.5	1.048	0.72
OM6	G1	059309	255946	22	7	217	47	315	13.22	5.9	1.040	0.55
OM7	G1	058533	255703	7	29	296	3	28	11.93	2.1	1.012	0.07
OM8	G1	059018	255290	13	39	220	51	41	10.59	4.9	1.034	–0.61
OM9	G1	058393	256620	15	25	248	31	354	10.68	4.7	1.032	0.55
OM10	G1	057766	256680	16	38	224	49	69	14.23	4.73	1.03	0.70
OM11	KIA	KIA	KIA	KIA	KIA	KIA	KIA	KIA	KIA	KIA	KIA	KIA
OM12	G1	058061	255442	21	14	218	51	111	4.18	3.5	1.023	–0.60
OM13	G1	057445	259756	17	41	210	48	17	11.60	8.2	1.050	0.28
OM14	G1	057275	258980	8	14	245	33	11	10.58	9.3	1.066	0.61
OM15	G1	058041	259001	19	40	241	9	339	12.31	5.1	1.035	0.59
OM16	G1	057372	258237	10	34	227	40	351	10.11	4.2	1.027	0.41
OM17	G2	056523	257658	18	40	225	39	358	11.73	7.6	1.060	0.84
OM18	G2	056637	257698	14	52	45	20	288	13.22	5.5	1.036	0.49
OM19	G3	056253	257916	20	28	213	41	331	1.32	6.5	1.043	0.50
OM20	G2	056470	258109	15	27	217	31	325	13.98	7.0	1.046	0.46
OM21	G1	056023	258863	19	42	238	47	43	5.44	8.3	1.049	–0.01
OM21B	G1	056023	258863	10	40	233	50	47	5.39	10.1	1.061	–0.13
OM22	G1	055407	258669	17	40	191	50	4	1.09	6.2	1.038	0.30
OM23	G3	055379	257629	14	37	101	36	338	4.11	5.8	1.034	0.06
OM24	KIA	KIA	KIA	KIA	KIA	KIA	KIA	KIA	KIA	KIA	KIA	KIA
OM25	G1	055396	256790	20	19	32	64	257	4.01	6.3	1.042	0.51
OM26	G1	055941	255044	4	51	9	39	175	17.42	2.5	1.015	–0.17
OM27	G1	055352	256014	19	24	43	5	135	15.40	4.5	1.029	0.38
OM28	KIA	KIA	KIA	KIA	KIA	KIA	KIA	KIA	KIA	KIA	KIA	KIA
OM29	G1	057505	255339	19	24	260	55	131	13.14	3.1	1.021	0.63
OM30	G1	057061	256183	11	66	271	18	135	8.89	1.3	1.007	–0.11
OM31	G1	056986	256800	20	11	219	69	98	11.34	3.9	1.028	0.70
OM32	G1	056189	256870	17	18	237	56	117	3.55	2.7	1.017	–0.39
OM33	KIA	KIA	KIA	KIA	KIA	KIA	KIA	KIA	KIA	KIA	KIA	KIA
OM34	G1	059332	256377	18	35	281	16	179	14.44	6.7	1.045	0.52
OM35	G1	059226	256366	13	31	243	59	65	10.23	4.6	1.028	0.31
OM36	G1	059376	256001	13	38	257	17	154	13.13	5.0	1.033	0.53
OM37	G1	059308	255900	15	24	240	51	116	16.68	4.5	1.030	0.48
OM38	KIA	KIA	KIA	KIA	KIA	KIA	KIA	KIA	KIA	KIA	KIA	KIA
OM39	G1	059158	255814	20	42	238	43	91	4.96	8.0	1.056	0.59
OM40	G1	059175	255761	12	29	239	51	104	10.41	4.0	1.023	0.03
OM41	G1	059131	255399	18	9	91	51	192	6.98	6.7	1.040	0.14
OM42	G1	057170	259324	20	18	216	52	331	17.82	8.5	1.062	0.68
OM43	G1	057017	259930	21	27	211	48	335	7.83	7.6	1.050	0.46
OM44	G1	058063	258990	20	60	240	16	359	12.55	9.0	1.054	–0.19
OM45	G1	058060	258991	19	67	8	23	185	14.18	8.5	1.051	0.17
OM46	KIA	KIA	KIA	KIA	KIA	KIA	KIA	KIA	KIA	KIA	KIA	KIA
OM47	G1	056862	257780	4	55	225	29	6	3.69	8.4	1.064	0.78
OM48	G1	056864	257786	12	35	220	36	340	13.25	6.9	1.047	0.56
OM49	G1	056804	258409	18	30	44	36	160	15.62	6.3	1.045	0.67
OM50	G1	056804	258410	20	42	69	3	162	1.92	4.3	1.026	0.27
OM51	G3	056232	257697	18	24	228	37	119	0.38	4.0	1.026	0.44
OM52 A	G3	056235	257471	8	41	221	28	338	1.53	4.0	1.029	0.75
OM52 B	G3	056235	257471	18	40	225	21	116	0.55	4.5	1.034	0.84
OM53	G3	056233	257489	17	28	230	55	10	1.13	5.4	1.037	0.55
OM54	G1	055302	258508	14	36	159	54	339	12.10	6.1	1.036	0.20
OM55	G1	054813	257622	20	28	94	45	332	15.04	6.4	1.038	–0.01
OM56	G1	054315	257065	18	33	81	36	322	14.25	6.8	1.043	–0.36
OM57	G1	058069	256291	16	12	207	77	51	5.72	5.4	1.033	–0.33
OM58 A	G1	057277	255740	11	25	230	24	128	14.33	2.8	1.017	0.07
OM58 B	G1	057277	255740	14	15	223	39	120	13.82	2.7	1.016	0.26
OM59	G1	056786	254806	10	29	30	35	142	10.19	3.9	1.025	–0.49

https://doi.org/10.1017/S1755691015000201 Published online by Cambridge University Press

Table 1 (continued)

Site ID	Facies	East	North	n	K3 Plunge	K3 Trend	K1 Plunge	K1 Trend	Km × 10^{-3}(SI)	H (%)	Pj	Tj
OM60	G1	055938	255055	12	55	36	21	159	12.74	5.1	1.030	0.03
OM61	G1	056407	256295	12	18	205	68	25	9.87	4.9	1.029	−0.05
OM62	KIA	KIA	KIA	KIA	KIA	KIA	KIA	KIA	KIA	KIA	KIA	KIA
OM63	G1	055855	255689	12	43	32	17	138	14.87	3.6	1.023	−0.49
OM64	G1	056341	255788	19	60	346	25	131	14.03	4.8	1.028	−0.01
OM65	G1	058285	255286	12	54	21	34	177	3.51	6.9	1.047	−0.57
OM66	G1	058273	255287	12	13	260	55	151	10.42	3.9	1.026	−0.55
OM67	KIA	KIA	KIA	KIA	KIA	KIA	KIA	KIA	KIA	KIA	KIA	KIA
OM68	G1	054527	257286	13	41	75	25	322	17.69	5.2	1.032	−0.35
OM69	G1	059034	255887	12	44	325	46	131	15.13	5.0	1.031	−0.36
OM70	G2	056308	258227	18	46	201	35	336	12.77	7.5	1.046	0.26
OM71	G2	056027	258109	15	11	236	69	356	6.68	5.8	1.035	−0.29
OM72	G3	055980	257990	12	14	205	21	110	0.24	1.6	1.011	0.62
OM73	G3	055955	257974	14	18	202	50	314	3.11	8.8	1.063	0.66
OM74	G3	055634	257957	13	13	186	40	287	3.15	5.8	1.036	0.35
OM75	G3	055931	257854	15	22	216	5	308	0.73	7.2	1.048	0.52
OM76	G2	055343	257884	16	3	205	73	306	0.17	1.2	1.007	0.27
OM77	G2	055274	258097	14	27	188	18	287	12.41	5.1	1.035	0.61
OM78	G1	058049	257822	12	43	223	19	332	14.35	6.1	1.045	0.76
OM79	G1	059249	256505	21	37	51	27	163	9.50	3.3	1.024	0.70
OM80	G1	059275	256446	19	33	239	7	145	12.46	5.0	1.039	0.89
OM81	G1	056025	256126	15	8	23	24	116	11.62	2.2	1.014	−0.49
OM82	G1	055631	256018	15	39	41	3	308	14.77	4.5	1.028	−0.35
OM83	G1	055861	255682	15	54	16	34	173	14.51	4.6	1.034	0.74
OM84	G1	055875	255696	14	35	255	31	141	12.31	3.9	1.028	−0.71
OM85	G1	056126	255507	15	13	59	75	210	6.34	8.9	1.053	−0.10
OM86	G1	056347	255210	11	31	215	15	315	1.74	5.8	1.041	0.64
OM87	G1	056552	254747	15	42	44	1	135	12.15	4.2	1.025	−0.66
OM88	G1	056145	254757	15	41	38	33	163	15.30	5.2	1.031	−0.15
OM89	G1	057075	254939	14	35	88	12	186	0.16	1.6	1.010	0.34
OM90	G1	056846	255128	15	5	209	77	98	4.70	2.8	1.016	−0.14
OM91	G1	057034	255931	14	15	29	45	134	12.64	2.7	1.016	−0.27
OM92	G1	058003	255762	7	59	267	27	121	13.81	3.7	1.022	−0.04
OM93	G1	058380	255581	15	50	355	34	192	9.76	4.6	1.027	0.08
OM94	G1	058769	255584	15	52	267	22	145	11.50	3.9	1.023	−0.06
OM95	G1	054447	257178	15	32	53	35	298	6.05	5.7	1.034	−0.14
OM96	G1	054445	257111	14	20	74	40	327	9.64	6.4	1.041	−0.44
OM97	G1	054917	257080	15	11	53	25	318	10.56	7.0	1.041	−0.04
OM98	G1	054607	257151	11	1	0	29	270	9.72	5.6	1.033	−0.17
OM99	G1	054397	257388	11	12	49	48	306	10.02	3.6	1.021	0.07
OM100	G1	054397	257388	11	47	88	34	312	15.78	5.8	1.039	−0.55
OM101	G1	054404	257296	14	24	73	37	323	10.11	5.3	1.037	−0.64
OM102	G1	054940	257399	15	33	65	36	306	3.19	6.8	1.040	−0.09
OM103	G1	054806	258208	14	50	150	40	331	11.64	6.5	1.038	0.06
OM104	G1	054895	257942	15	51	110	35	321	14.94	5.2	1.031	0.04
OM105	G1	056584	259040	15	32	205	51	346	15.40	7.8	1.049	0.33
OM106	G3	052218	257726	15	35	93	35	335	5.08	6.7	1.041	0.27
OM107	G3	052344	257784	15	39	86	46	298	3.35	6.3	1.040	0.43
OM108	G2	052571	257776	15	39	97	34	335	10.16	4.4	1.026	−0.18
OM109	G1	054106	255307	13	21	39	7	132	14.55	7.1	1.048	0.53
OM110	G3	053013	255162	12	18	42	7	134	1.41	6.5	1.042	0.41
OM111	G3	053260	255103	12	17	57	72	221	1.09	5.0	1.030	0.22
OM112	G2	053584	254934	10	1	44	46	136	2.45	3.8	1.025	0.45
OM113	G1	053426	257108	13	47	87	34	312	14.34	5.4	1.033	−0.24
OM114	G1	054217	259871	13	54	183	35	347	12.63	6.5	1.040	0.26
OM115	G1	054777	259004	9	35	163	55	344	12.64	4.9	1.032	−0.44
OM116	G1	055231	259304	8	6	213	79	336	5.06	5.7	1.044	0.82
OM117	G1	056417	259694	13	39	223	6	317	12.02	6.7	1.049	0.67

https://doi.org/10.1017/S1755691015000201 Published online by Cambridge University Press

Table 2 Summary of AMS results

	All Sites (n = 113)				
Parameter	**Tj**	**Pj**	**lnPj**	**H (%)**	**K × 10^{-6}(SI)**
Min	−0.71	1.01	0.007	1.17	166
Max	0.95	1.07	0.064	10.12	17819
Mean	0.2	1.04	0.03	5.33	9688
Std. Dev	0.42	0.013	0.012	1.83	4938
G1 (n = 90)					
Min	−0.71	1.01	0.007	1.28	1119
Max	0.95	1.066	0.064	10.12	17819
Mean	0.14	1.03	0.034	5.3	10934
Std. Dev	0.435	0.013	0.012	1.84	4138
G2 (n = 9)					
Min	−0.29	1.01	0.007	1.17	166
Max	0.84	1.06	0.058	7.63	13975
Mean	0.32	1.04	0.035	5.32	9285
Std. Dev	0.34	0.014	0.014	1.94	4746
G3 (n = 14)					
Min	0.002	1.01	0.01	1.55	244
Max	0.016	1.06	0.06	8.76	5082
Mean	0.011	1.03	0.036	5.58	1941
Std. Dev	0.004	0.011	0.011	1.68	1472

between 7 and 22 (average 15) 21 mm x 25 mm right-cylindrical sub-specimens were analysed per sample site. A greater number of sites were sampled in localities close to facies contacts and shear zones. One in every twenty block samples were collected as duplicates as part of an AMS comparative study. A suite of rock magnetic experiments were also carried out to determine rock magnetic mineralogy, results and procedures of which are included in the online supplementary data section (see Appendix – Supplementary Magnetic Data).

3.1. AMS results

Results from a total of 113 out of 121 sample sites were accepted (Table 1); data from eight sites were rejected owing to localised hydrothermal overprinting. A summary of AMS data compiled from each facies is presented in Table 2. A review of the parameters used to evaluate the AMS tensor can be found in Tarling & Hrouda (1993); here, the principal parameters used to characterise magnetic anisotropy are:

$$K_m = [K1 + K2 + K3]/3 \quad (1)$$

$$P_j = \{\exp\sqrt{2}[(\square 1 - \square)2 + (\square 2 - \square)2 + (\square 3 - \square)2]\} \quad (2)$$

$$T_j = [2\square 2 - \square 1 - \square 3]/[\square 1 - \square 3] \quad (3)$$

$$H = [K1 - K3]/K_{mean} \quad (4)$$

where K_m is the mean susceptibility, P_j and T_j are the Corrected Anisotropy Degree and the Shape Factor respectively (Jelinek 1981) and H is the Total Anisotropy (Owens 1974). The T_j parameter is used to distinguish oblate ($0 < T_j < 1$) from prolate fabrics ($0 > T_j > -1$) (Jelinek 1981). The shape of highly oblate AMS tensors (i.e., a magnetic foliation) can be visualised as a flattened ellipsoid in the K1–K2 plane ($K3 \ll K2 \approx K3$). In this scenario, sub-samples return comparable K3 axes orientations (normal to the plane), while K1–K2 axes are distributed along the plane of flattening. Where the AMS tensor is highly prolate ($K1 \gg K2 \approx K3$), sub-specimen K1 susceptibility axes cluster and a girdle may be defined by K2 and K3 axes. Both a lineation and foliation can be determined where all principal susceptibility axes are well defined. If a composite fabric is present, or where an intermediate fabric occurs due to structural overprinting, the stereograph projection of the AMS tensor commonly shows broad 95 % confidence ellipses and a low degree of consistency between normalised and un-normalised stereograph tensor projections (Owens 2000).

AMS results yield mean susceptibility (K_{mean}) values that vary from 0.166×10^{-3} to 17.82×10^{-3} (SI units) across the pluton (mean $= 9.69 \times 10^{-3} \pm 4.94 \times 10^{-3}$). A sharp contrast in K_{mean} values is noted between earlier ($G1 = 10.93 \times 10^{-3}$; $G2 = 9.29 \times 10^{-3}$) and later ($G3 = 1.94 \times 10^{-3}$) facies (Table 2). A contour map of K_{mean} (Fig. 8a) reveals a low magnetic anomaly over the Aughrus Peninsula, Friar Island and Curagh Island which coincides with the mapped extent of the G3 facies. There is a similar, but less apparent, anomaly associated with the extent of the G2 facies. The corrected degree of anisotropy (P_j) varies between 1.01 and 1.07 (mean = 1.04 ± 0.013), and the overall Degree of Anisotropy (H) varies between 1.2 % and 10.1 % (mean = 5.33 % ± 1.8 %). The maximum variance of mean P_j and H values between each facies is 0.01 % and 0.28 % respectively. As illustrated by a contour map of P_j (Fig. 8b), these data show that magnetic anisotropy does not systematically vary across facies contacts. The same observation is made for T_j values; G1 and G2 samples exhibit a spectrum of AMS ellipsoid shapes that range from well-defined oblate (−0.71), to tri-axial to strongly prolate (0.95) (Table 2). Samples taken from G3 return only weak to moderate oblate ellipsoids (T_j min = 0.0024; max = 0.016) and adjacent G2 and G1 sites also return similar shape and strength of anisotropy parameters. These data show that K_{mean} systematically fluctuates across facies contacts and is controlled by the relative concentration of magnetite in each facies, and that magnetic anisotropy is not inherent to granite facies.

A map of the compiled AMS data, with representative stereographic projections of averaged AMS ellipsoids (95 % confidence ellipse), is presented in Figure 9. Either lineations

https://doi.org/10.1017/S1755691015000201 Published online by Cambridge University Press

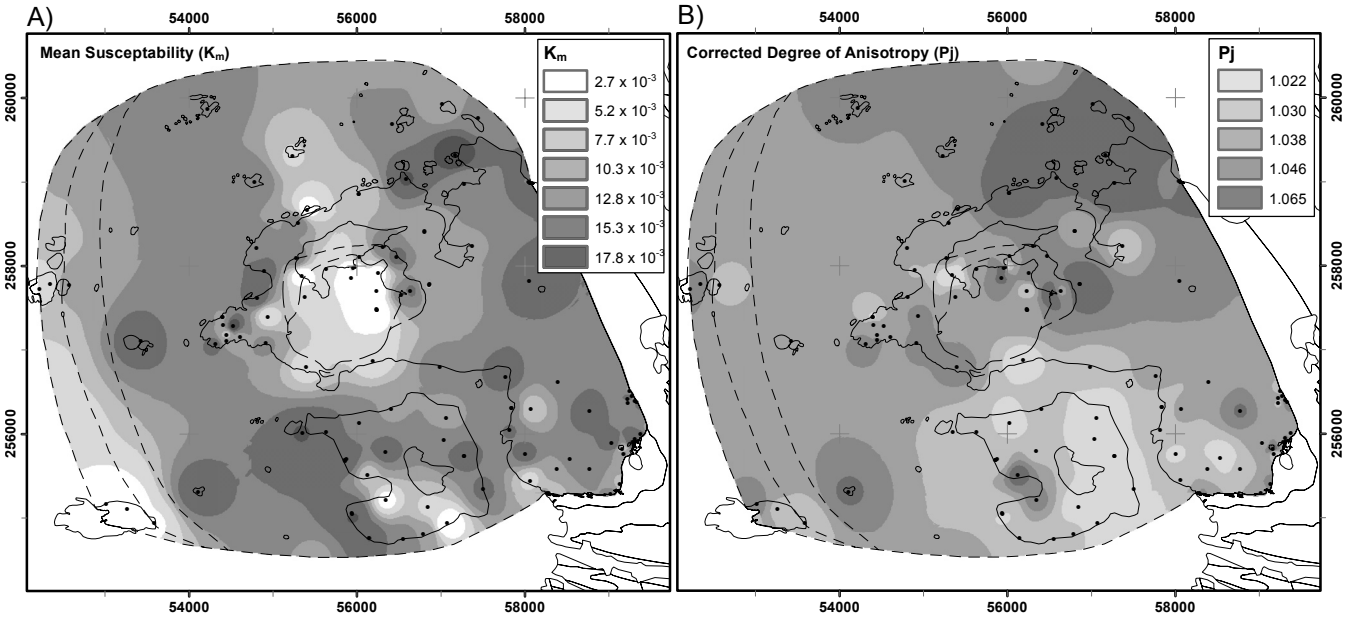

Figure 8 (a) Contour map showing magnetic susceptibility (K_{mean}) remains $\geq 10^{-3}$ SI across the pluton. (b) A contour map of Corrected Degree of Anisotropy (P_j) shows no relationship between facies contacts and the degree of anisotropy.

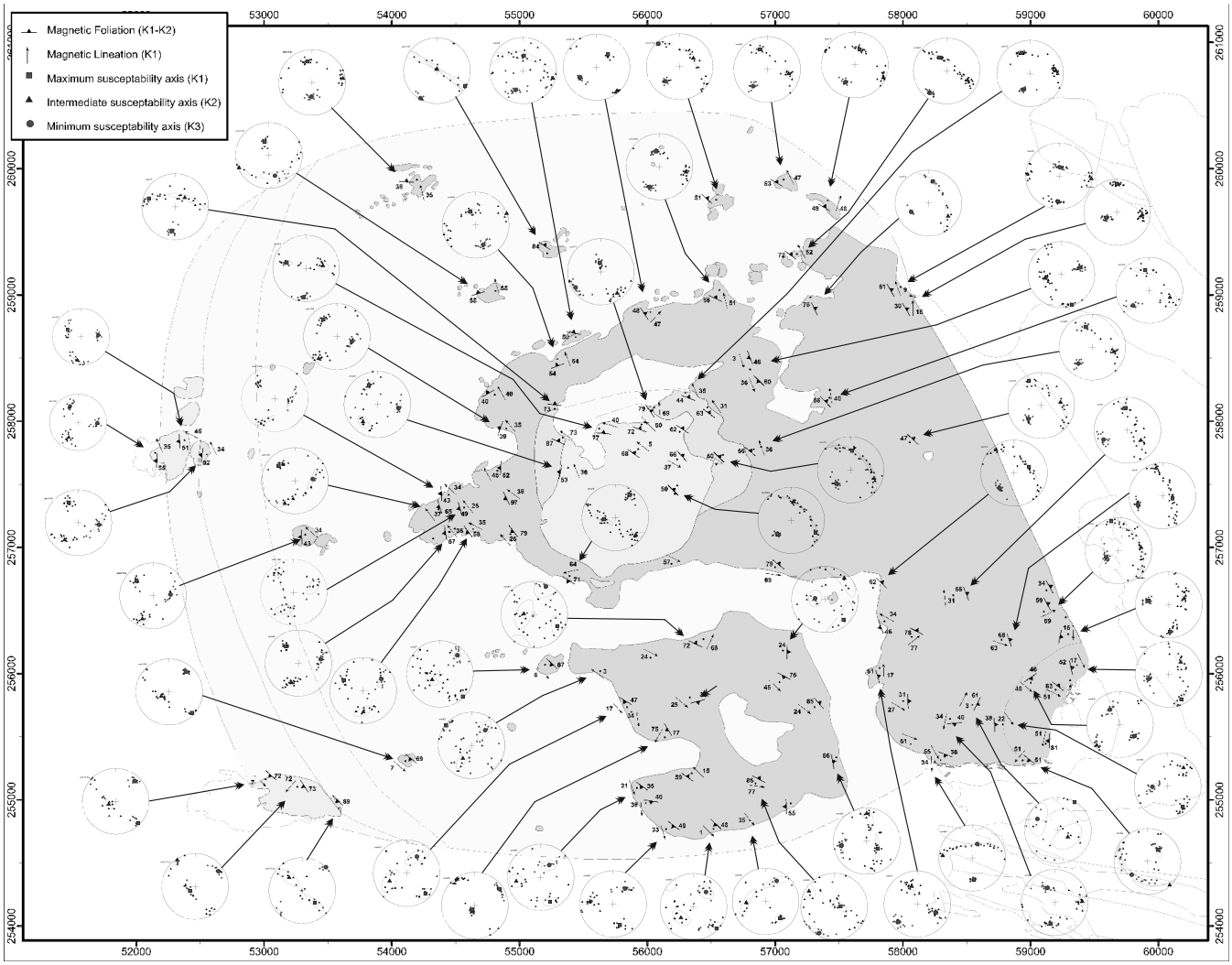

Figure 9 Results of AMS analysis with representative southern hemisphere projections of averaged AMS tensors. Each data point is plotted as a foliation, lineation or both, depending on calculated anisotropy values.

https://doi.org/10.1017/S1755691015000201 Published online by Cambridge University Press

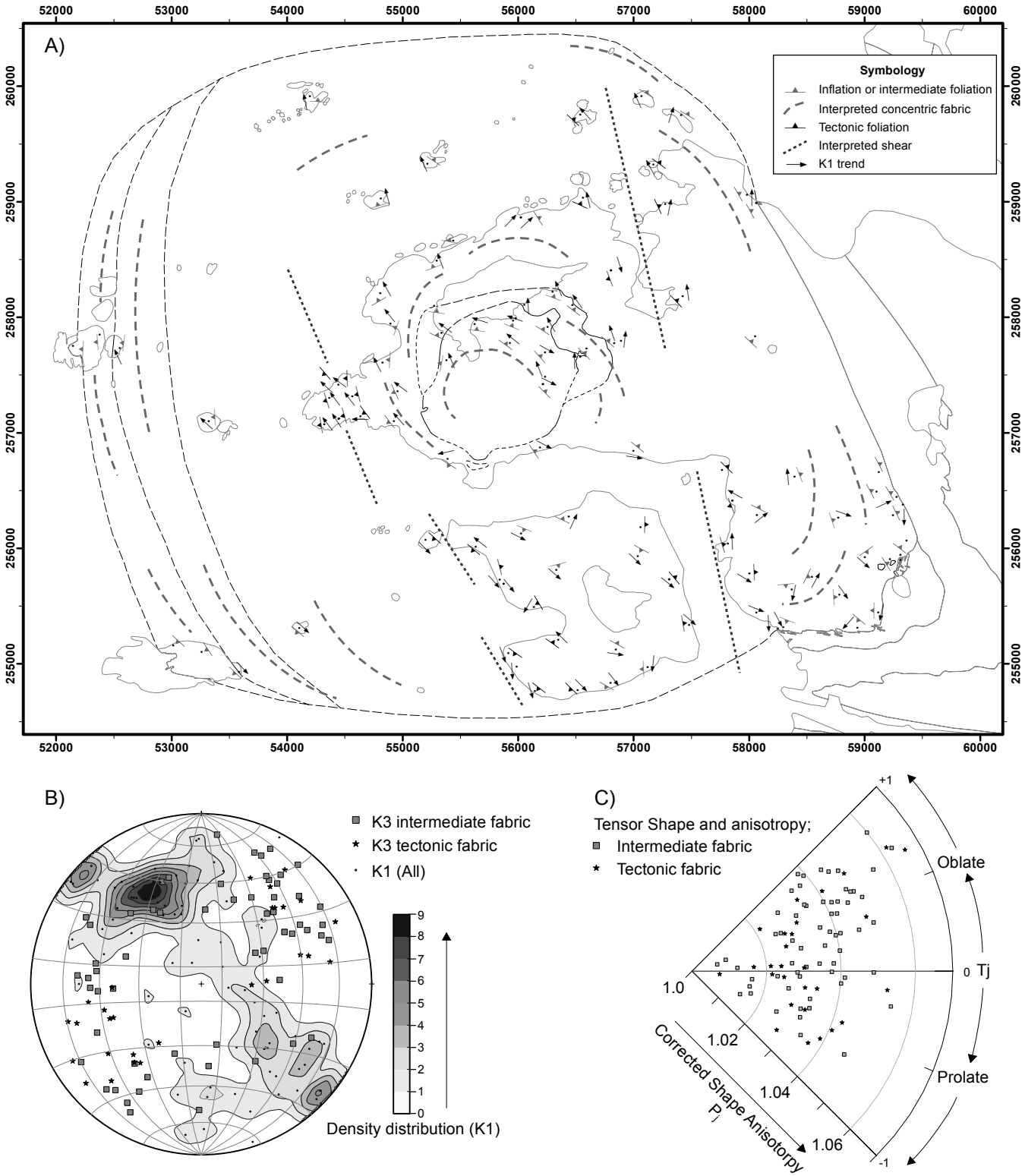

Figure 10 A summary of AMS data shows that the concentric foliation is cross-cut by NNW–SSE tectonic shear zones. (A) Two sets of fabrics are identified: (1) concentric foliations, associated with laccolith inflation; and (2) cross-cutting NNW–SSE foliations, attributed to submagmatic shearing along NNW–SSE shear zones (labelled 'tectonic foliation'). (B) A polar plot of all AMS data points shows that K1 axes are aligned parallel to NNW–SSE axes. 'Tectonic foliation' K3 axes show a very consistent NNW–SSE subvertical foliation orientation. A much broader distribution of 'inflation foliation' K3 axes reflects the concentric fabric which was partially overprinted by tectonic shearing. (C) Polar plot of Tj vs Pj data shows the spectrum of AMS tensors detected across the pluton.

or foliations are plotted from sites where strongly oblate or prolate tensors were detected; both symbols are used for sites where both a magnetic lineation and foliation were detected.

A summary of AMS data is presented in Figure 10. Two distinct AMS foliation patterns are identified (Fig. 10a). At the core of the intrusion, moderately-inclined, outward-dipping oblate fabrics define a strong concentric pattern. In the east of the pluton, where the granite is in contact with the Lakes Marble Formation and the Streamstown Schist Formation, foliations strike contact-parallel and are slightly oblique to the orientation of the host rock structure. Similarly, on Friar Island and Cruagh Island, magnetic foliations dip moderately

https://doi.org/10.1017/S1755691015000201 Published online by Cambridge University Press

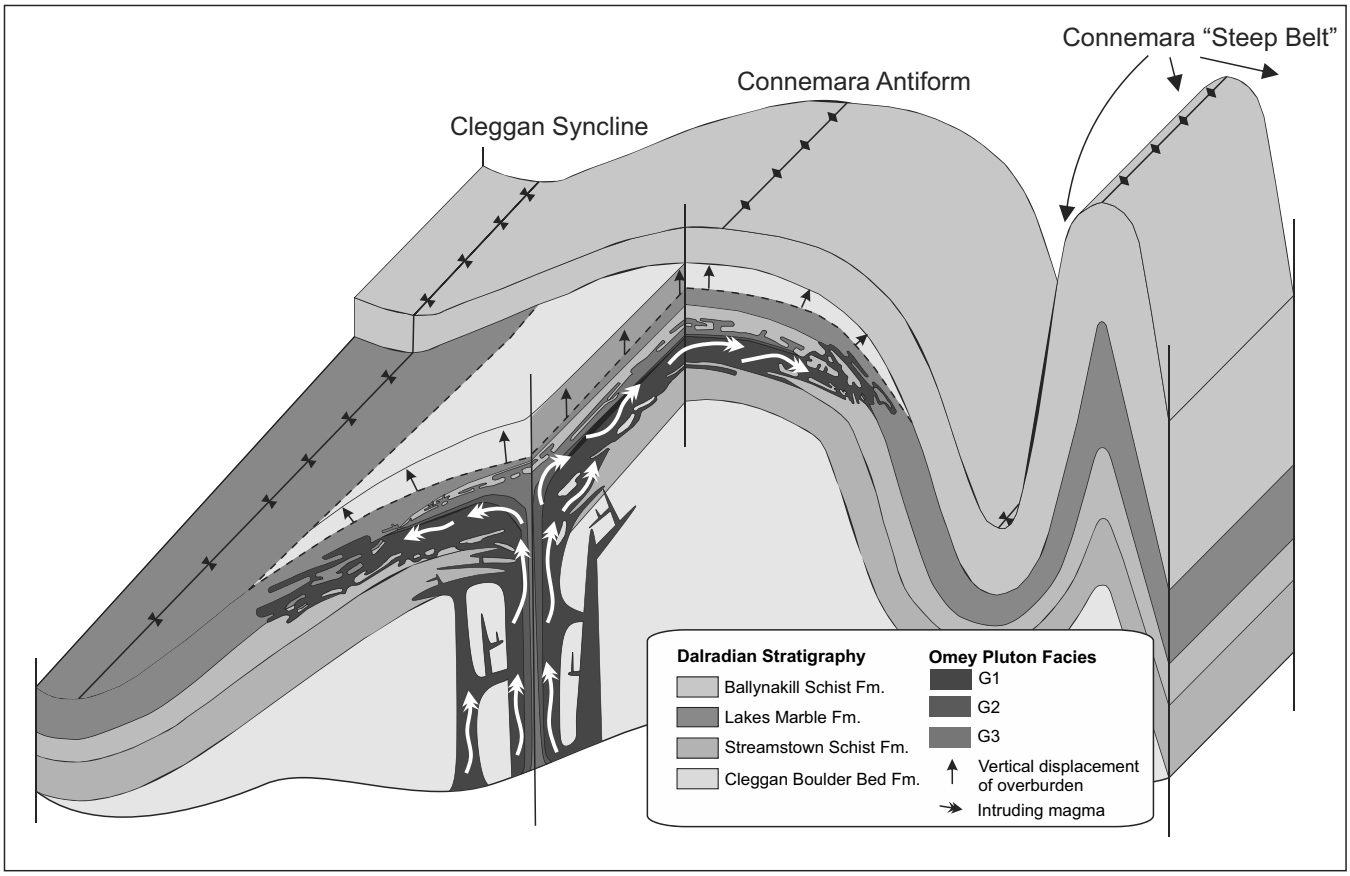

Figure 11 Block diagram depicting the overall symmetry of the Omey Pluton, which intruded along, and partially pseudomorphed, the Connemara Antiform.

outwards and are overall contact-parallel, but are often oblique to the local sheeted intrusions which intrude parallel to compositional layers in the folded host rock. Therefore, AMS data contrast field observations that clearly indicate that magma sheeted into the country rock along the folded limbs of the D4 Connemara Antiform and pre-granite regional joint sets. We interpret these magnetic foliations as inflation fabrics which represent the forceful input of magma into the pluton; an observation consistent with interpretations made on data derived from similar intrusions (Molyneux & Hutton 2000; Hutton & Siegesmund 2001).

A different set of magnetic foliations are identified in close proximity to faults which have been identified by field mapping and petrographic observations (Fig. 10a). Magnetic foliations in these areas strike NNW–SSE, are discordant to internal and external pluton contacts, are steeply inclined and become more intense within the NNW–SSE fault zones. K1 vectors, i.e., magnetic lineations, maintain an overall NNW–SSE trend across the pluton and exhibit the highest anisotropy within the NNW–SSE fault zones. A stereographic projection of all AMS data shows that K3 axes from samples spatially associated with shear zones are tightly clustered in the ESE and WSW of the stereonet, while K3 axes sampled >250 m from the fault zones define a concentric pattern and are more evenly distributed (Fig. 10b). K1 axes throughout the pluton consistently plot along a NNW–SSE axis, regardless of proximity to faults (Fig. 10b).

Several examples of magnetic fabrics which bear no immediate relationship to either concentric or NNW–SSE fabrics are noted on Omey Island and immediately east in the Fountain Hill area (Fig. 9). The discordant nature of the mean tensor relative to geological contacts, the contrasting normalised and un-normalised AMS tensor projections, and the broad 95 % confidence ellipse (Owens 2000), indicate that these are structurally intermediate fabrics and may be the result of interaction between shearing along less prominent E–W faults and inflation fabrics or NNW–SSE shear structures.

4. Discussion

New field observations place rigorous stratigraphical controls on the position of the Omey Pluton and, having established the orientation of the pluton's contacts, the overall symmetry of the intrusion can be constrained. The stratigraphy of the host rocks young to the E, the Cleggan Boulder Bed Formation being the oldest and the Lakes Marble Formation the youngest (Leake & Tanner 1994). The attitude of external contacts closely parallels the symmetry of the Connemara Antiform. Along the hinge, the granite contact dips gently to the E parallel to the plunge of the fold. The base of the sheet intrudes the Cleggan Boulder Bed Formation and a discordant roof is defined by the Streamstown Schist Formation and the Lakes Marble Formation. The northern and southern contacts are bound by, and are generally parallel to, the orientation of the fold limbs, as are internal facies boundaries. Thus, the architecture of this sheeted intrusion clearly pseudomorphs the symmetry of the Connemara Antiform into which it was emplaced, giving the body a phacolithic structure (Harker 1909; Corry 1988). However, as several examples of highly discordant external contacts have been described, the term 'discordant phacolith' is proposed to best describe the overall geometry (Fig. 11).

https://doi.org/10.1017/S1755691015000201 Published online by Cambridge University Press

4.1. Interplay between pluton ballooning and tectonic stretching fabrics

In apparently undeformed granitoid samples, where there is no textural evidence for tectonic deformation, magnetic lineations in igneous rocks are often taken to reliably indicate magma flow direction and are therefore used to model magma transport mechanisms (Petronis *et al.* 2004; Stevenson *et al.* 2008; Magee *et al.* 2012). Parés & van der Pluijm (2002) show that in rocks with a weak initial foliation, magnetic lineations are highly sensitive to the extension direction of the finite strain ellipsoid, and conclude that the final AMS tensor is largely dependent on the nature of an original fabric, rather than a direct reflection of the bulk strain ellipsoid. Accordingly, subtle primary flow fabrics in granitoid plutons are more susceptible to overprinting by later processes such as pluton inflation (Baxter *et al.* 2005; McCarthy *et al.* 2015), tectonic stretching (Kligfield *et al.* 1981; Alimohammadian *et al.* 2013) and hydrothermal alteration (Just & Kontny 2011; Valley *et al.* 2011). Petronis *et al*. (2012) interpret AMS data from the Ross of Mull Granite, Scotland, as a magma flow fabric which is partially overprinted by tectonic shearing because the magnetic lineation strikes parallel to well-known regional faults which were active during and after magma intrusion. Benn *et al.* (2001) exploit the sensitivity of the AMS technique and emphasises its use as a viable strain marker in syntectonic plutons, rather than as a magma flow indicator.

Concentric foliations, interpreted here as inflation fabrics, within the Omey Pluton are subtle (H most often <9 %), and thus are highly sensitive to tectonic stretching, particularly prior to full crystallisation of magma. Field observations and AMS data also identify two sets of shear zones (NNW–SSE and ENE–WSW), which are defined by: (i) abrupt breaks in topography; (ii) submagmatic foliations within 5 m-wide shear zones (later reactivated as faults); (iii) the NNW–SSE and E–W alignment of late Caledonian & Carboniferous mafic dykes within these shear zones; and (iv) the common alignment of AMS K1 axes that cross-cut all mapped facies contacts. The key observation made here is that the azimuth of AMS K1 axes is strikingly consistent across the entire pluton. Although the majority of these samples show an apparent lack of deformation, K1 reliably parallels apparently discrete and localised NNW–SSE shear zones. The detected lineations are therefore interpreted to be a product of tectonic stretching that was concurrent with, or followed immediately, after pluton inflation, and do not represent primary magma flow features, even in areas that appear to be undeformed.

4.2. Structural control over magma ascent

Prominent NNW–SSE shear zones within the Omey Pluton lie parallel to regional D5 faults that cross-cut the Connemara Metamorphic Complex and predate the Omey Pluton (Fig. 1; see also Leake & Tanner 1994). Similar NNW–SSE faults facilitated magma ascent during the construction of the Roundstone Pluton, thus showing that these faults were exploited as ascent conduits at $\sim$420 Ma. We argue that the suite of NNW–SSE faults that cross-cut the Omey Pluton are inherently related to those parallel structures that are observed in the country rock, with which these structures share a similar kinematic history.

The concentric arrangement of granite facies around the centre of the pluton suggests centralised ascent, but sub-lateral sheeting of magma intruding from the east or west is also possible. The G3 facies occurs near the roof of the intrusion on Aughrus More and on the islands offshore to the west (Fig. 2). The fact that G3 does not occur adjacent to the fold axis in the east suggests that this facies did not intrude from the west but more likely from the centre of the pluton, and then sheeted laterally up-dip along the fold axis of the Connemara Antiform towards the west. In light of the temporal coincidence of magma transport to the site of emplacement and fault reactivation, we propose that ascent was achieved within a sub-vertical central conduit. In this scenario, the onset of regional sinistral transpression at $\sim$425 Ma caused vertical axis rotation of fault blocks bound by NNW–SSE and E–W faults that are observed in the field (Fig. 12). Dilation focused at fault junctions facilitated magma ascent, similar to the mechanisms envisaged by Jacques & Reavy (1994). At the site of emplacement, magma intruded laterally into the folded country rock along bedding and joint planes, to produce an overall discordant phacolith, and continued forceful injection of magma formed a subtle concentric pure shear inflation fabric. Both NNW–SSE and E–W faults were subsequently reactivated due to late Caledonian tectonism and, during the Carboniferous, as conduits for relatively minor intrusions.

5. Regional significance

Earlier investigations on the structural controls over the GGC, and the influence of regional stress have focused exclusively on the Main Batholith; a consensus that magma was emplaced at $\sim$400 Ma along a zone of dilation within the Skird Rocks Fault due to regional sinistral transtension has been reached (Desouky *et al.* 1996; Baxter *et al.* 2005; Leake 2008; Feely *et al.* 2007). However, the structural relationship between the Earlier Plutons and the Main Batholith has not, as of yet, been considered.

We propose that anticlockwise vertical axis rotation of fault blocks within the Connemara Metamorphic Complex during regional transpression controlled the siting of the Earlier Plutons along NNW–SSE faults. Regional far field stress evolved from orogenic orthogonal shortening to sinistral oblique compressive stress between 430 Ma and 425 Ma (Dewey & Strachan 2003). In western Ireland, the Connemara terrane represents a deformation zone bound by the Highland Boundary Fault (HBF) and the Skird Rocks Fault (SRF), along which sinistral transpressive strike slip occurred. The deformation zone, bound by these faults, was structurally heterogeneous and decoupled along strike due to strain partitioning along NNW–SSE faults (e.g. the Clifton–Mace Fault and the Barna Fault (Fig. 12)). Regional transpression promoted anti-clockwise rotation of the terrane block bound by the Clifton Mace Fault, the Barna Fault, the Skird Rocks Fault and the Highland Boundary Fault (or splay of) (Fig. 12). Thus, local dextral transtensive stress is predicted along NNW–SSE faults, while the HBF and SRF were in the compressive field. As a consequence, NNW–SSE faults presented a favourable migration conduit for ascending magma throughout regional transpression. The Omey and Roundstone Plutons were emplaced during this time and are cited over NNW–SSE faults known to have been active at this time. We suggest that these supplied magma to the upper crust and that emplacement was controlled by local factors, namely the symmetry of the Connemara Antiform (this study) and the Mannin Thrust (McCarthy *et al.* 2015), respectively.

In contrast, the overall shape and internal architecture of the Main Batholith is dominated by WSW–ENE trending structures (Desouky *et al.* 1996; Crowley & Feely 1997; Baxter *et al.* 2005; Leake 2008). This observation suggests that magma ascent was controlled by the Skird Rocks Fault, which is predicted to have undergone net extension during regional

https://doi.org/10.1017/S1755691015000201 Published online by Cambridge University Press

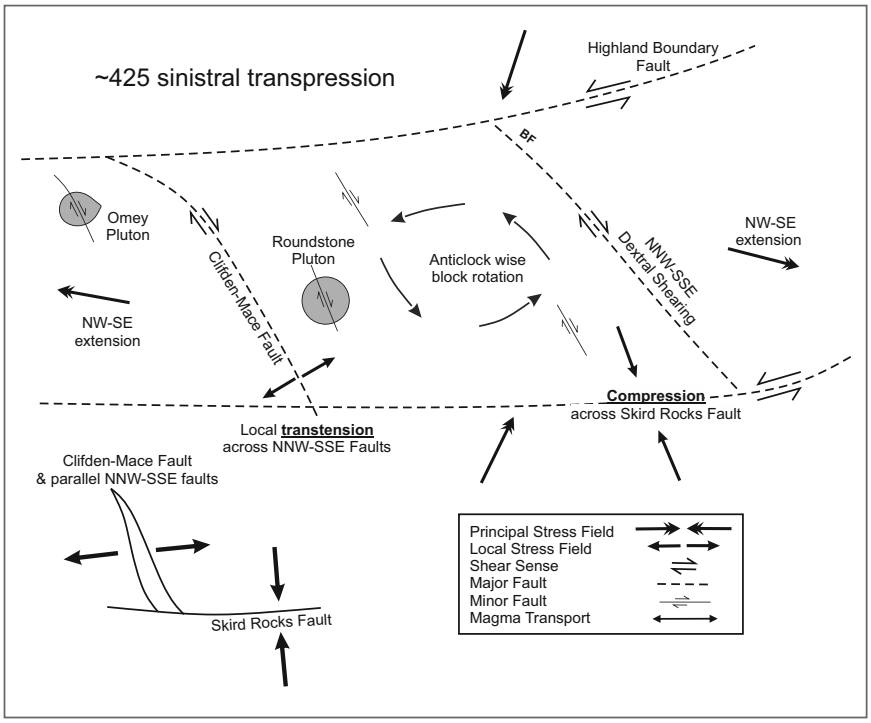

Figure 12 A schematic model depicting the interplay between regional stress, local structures and magma ascent. Anticlockwise vertical axis block rotation, triggered by regional transpression, leads to dilation along NNW–SSE conduits.

transtension, thus making it a more favourable magma transport conduit during orogenic collapse at ~400 Ma.

6. Conclusions and further work

The control of large faults on magma transport in the crust is a long-standing concept (Richey 1932; Pitcher & Bussell 1977). The interplay between such structures and evolving regional stress fields during magmatism has been demonstrated in several case studies (Jacques & Reavy 1994; Hutton & Alsop 1996; Brown & Solar 1998; Pe-Piper *et al.* 2002). For example, research in Donegal (Hutton & Alsop 1996; Stevenson *et al.* 2008) has shown how the construction of the Donegal Batholith was ultimately controlled by the interactions of two major crustal structures, the Donegal Lineament and the Main Donegal Shear Zone. It now appears that a similar situation pertains to the Galway Granite Complex, whereby the orientation of fault systems relative to the regional stress field during magmatism dictated which structures were utilised as magma conduits during pluton construction.

The current work shows that the oldest known pluton of the GGC (Omey) was controlled by a NNW–SSE fault system and that it shares certain structural relationships with the Roundstone Pluton which intruded at approximately the same time, at ~420 Ma (McCarthy *et al.* 2015). In contrast, the Main Batholith intruded into the WNW–ESE Skird Rocks Fault much later, at 400 Ma. This implies that a kinematic transition, i.e., transpression to transtension, occurred during construction of the complex, which led to structures in different orientations being exploited as magma conduits over time. If correct, this hypothesis predicts that plutons of a similar age which were intruded into comparable kinematic regimes will exhibit predictable structural controls.

7. Acknowledgements

We would like to thank the local community at Claddaghduff, Co. Galway, and Ruth and Jon Hunt for their continued hospitality. Martin Feely is thanked for helpful discussions. WMcC acknowledges receipt of an Irish Research Council for Science Engineering and Technology (IRCSET) grant and a National University of Ireland Travelling Studentship for postgraduate study at University College Cork.

8. Appendix – Supplementary Magnetic Data

The supplementary magnetic data, describing in detail the investigation of rock magnetic properties for AMS interpretation, are published with the online version of this paper. This is hosted by the Cambridge Journals Online (CJO) service and can be viewed at http://journals.cambridge.org/tre

9. References

Ahmed-Said, Y. & Leake, B. E. 1996. The conditions of metamorphism of a grossular–wollastonite vesuvianite skarn from the Omey Granite, Connemara, western Ireland, with special reference to the chemistry of vesuvianite. *Mineralogical Magazine* **60**, 541–50.

Alimohammadian, H., Hamidi, Z., Aslani, A., Shahidi, A., Cifelli, F. & Mattei, M. 2013. A tectonic origin of magnetic fabric in the Shemshak Group from Alborz Mts. (northern Iran). *Journal of Asian Earth Sciences* **73**, 419–28.

Badley, M. E. 1976. Stratigraphy, structure and metamorphism of Dalradian rocks of the Maumturk Mountains, Connemara, Ireland. *Journal of the Geological Society, London* **132**, 509–20.

Baxter, S., Graham, N. T., Feely, M., Reavy, R. J. & Dewey, J. F. 2005. A microstructural and fabric study of the Galway Granite, Connemara, western Ireland. *Geological Magazine* **142**, 81–95.

https://doi.org/10.1017/S1755691015000201 Published online by Cambridge University Press

Benn, K., Paterson, S. R., Lund, S. P., Pignotta, G. S. & Kruse, S. 2001. Magmatic fabrics in batholiths as markers of regional strains and plate kinematics: example of the Cretaceous Mt. Stuart batholith. *Physics and Chemistry of the Earth, Part A: Solid Earth and Geodesy* **26**, 343–54.

Brown, M. & Solar, G. S. 1998. Granite ascent and emplacement during contractional deformation in convergent orogens. *Journal of Structural Geology* **20**, 1365–93.

Brown, P. E., Ryan, P. D., Soper, N. J. & Woodcock, N. H. 2008. The Newer Granite problem revisited: a transtensional origin for the Early Devonian Trans-Suture Suite. *Geological Magazine* **145**, 235–56.

Buchwaldt, R., Kroner, A., Toulkerides, T., Todt, W. & Feely, M. 2001. Geochronology and Nd–Sr systematics of late Caledonian granites in western Ireland: new implications for the Caledonian Orogeny. *Geological Society of America Abstracts with Programs* **33**(1), A32.

Cobbing, E. J. 1969. The Geology of the District Northwest of Clifden, Co. Galway. *Proceedings of the Royal Irish Academy. Section B: Biological, Geological and Chemical Science* **67**, 303–25.

Corry, C. E. 1988. Laccoliths: Mechanics of emplacement and growth. *Geological Society of America Special Paper* **220**, 3–10.

Crowley, Q. & Feely, M. 1997. New perspectives on the order and style of granite emplacement in the Galway Batholith, western Ireland. *Geological Magazine* **134**, 539–48.

Desouky, M. E., Feely, M. & Mohr, P. 1996. Diorite-granite magma mingling and mixing along the axis of the Galway Granite batholith, Ireland. *Journal of the Geological Society, London* **153**, 361–74.

Dewey, J. F. & Strachan, R. A. 2003. Changing Silurian–Devonian relative plate motion in the Caledonides: sinistral transpression to sinistral transtension. *Journal of the Geological Society, London* **160**, 219–29.

Elias, E. M., Macintyre, R. M. & Leake, B. E. 1988. The cooling history of Connemara, western Ireland, from K-Ar and Rb-Sr age studies. *Journal of the Geological Society, London* **145**, 649–60.

Feely, M., Coleman, D., Baxter, S. & Miller, B. 2003. U–Pb zircon geochronology of the Galway Granite, Connemara, Ireland: implications for the timing of late Caledonian tectonic and magmatic events and for correlations with Acadian plutonism in New England. *Atlantic Geology* **39**, 175–84.

Feely, M., Selby, D., Conliffe, J. & Judge, M. 2007. Re–Os geochronology and fluid inclusion microthermometry of molybdenite mineralisation in the late-Caledonian Omey Granite, western Ireland. *Applied Earth Science* **116**, 143–49.

Feely, M., Selby, D., Hunt, J. & Conliffe, J. 2010. Long-lived granite-related molybdenite mineralization at Connemara, western Irish Caledonides. *Geological Magazine* **147**, 886–94.

Ferguson, C. C. & Al-Ameen, S. I. 1986. Geochemistry of Dalradian pelites from Connemara, Ireland: new constraints on kyanite genesis and conditions of metamorphism. *Journal of the Geological Society, London* **143**, 237–52.

Ferguson, C. C. & Harvey, P. K. 1979. Thermally overprinted Dalradian rocks near Cleggan, Connemara Western Ireland. *Proceedings of the Geologists' Association* **90**, 43–50.

Friedrich, A. M., Hodges, K. V, Bowing, S. A. & Martin, M. W. 1999a. Geochronological constraints on the magmatic, metamorphic and thermal evolution of the Connemara Caledonides, western Ireland. *Journal of the Geological Society, London* **156**, 1217–30.

Friedrich, A. M., Bowring, S. A., Martin, M. W. & Hodges, K. V. 1999b. Short-lived continental magmatic arc at Connemara, western Irish Caledonides: implications for the age of the Grampian orogeny. *Geology* **27**, 27–30.

Graham, N. T., Feely, M. & Callaghan, B. 2000. Plagioclase-rich microgranular inclusions from the late-Caledonian Galway Granite, Connemara, Ireland. *Mineralogical Magazine* **64**, 113–20.

Harker, A. 1909. *The Natural History of Igenous Rocks*. New York: Macmillan. 384 pp.

Hutton, D. H. W. 1988. Granite emplacement mechanisms and tectonic controls: inferences from deformation studies. *Transactions of the Royal Society of Edinburgh*: *Earth Sciences* **79**, 245–55.

Hutton, D. H. W. 2009. Insights into magmatism in volcanic margins: bridge structures and a new mechanism of basic sill emplacement – Theron Mountains, Antarctica. *Petroleum Geoscience* **15**, 269–78.

Hutton, D. H. W. & Alsop, G. I. 1996. The Caledonian strike-swing and associated lineaments in NW Ireland and adjacent areas: sedimentation, deformation and igneous intrusion patterns. *Journal of the Geological Society, London* **153**, 345–60.

Hutton, D. H. W. & Siegesmund, S. 2001. The Ardara Granite: Reinflating the Balloon Hypothesis. *Zeitschrift der Deutschen Geologischen Gesellschaft* **152**, 309–23.

Jacques, J. M. & Reavy, R. J. 1994. Caledonian plutonism and major lineaments in the SW Scottish Highlands. *Journal of the Geological Society*, *London* **151**, 955–1060.

Jelinek, V. 1981. Characterization of the magnetic fabric of rocks. *Tectonophysics* **79**, T63–T67.

Just, J. & Kontny, A. 2011. Thermally induced alterations of minerals during measurements of the temperature dependence of magnetic susceptibility: a case study from the hydrothermally altered Soultz-sous-Forêts granite, France. *International Journal of Earth Sciences* **101**, 819–39.

Kilburn, C., Shackleton, R. M. & Pitcher, W. S. 1965. The stratigraphy and origin of the portaskaig boulder bed series (Dalradian). *Geological Journal* **4**, 343–60.

Kinahan, G. H. 1869. Explanation to accompany Sheet 105 with that portion of Sheet 114 that lies north of Galway Bay. *Memoir of the Geological Survey of Ireland, Dublin*.

Kinahan, G. H. 1878. Explanatory memoir to accompany Sheets 93 and 94, with the adjoining portions of Sheets 83, 84, and 103, of the maps of the Geological Survey of Ireland. *Memoir of the Geological Survey of Ireland, Dublin*.

Kligfield, R., Owens, W. H. & Lowrie, W. 1981. Magnetic susceptibility anisotropy, strain, and progressive deformation in Permian sediments from the Maritime Alps (France). *Earth and Planetary Science Letters* **55**, 181–89.

Leake, B. E. 1974. The crystallization history and mechanism of emplacement of the western part of the Galway Granite, Connemara, Western Ireland. *Mineralogical Magazine* **39**, 498–513.

Leake, B. E. 1986. The geology of SW Connemara, Ireland: a fold and thrust Dalradian and metagabbroic-gneiss complex. *Journal of the Geological Society, London* **143**, 221–36.

Leake, B. E. 2008. Mechanism of emplacement and crystallisation history of the northern margin and centre of the Galway Granite, western Ireland. *Transactions of the Royal Society of Edinburgh: Earth Sciences* **97**(for 2006), 1–23.

Leake, B. E. 2011. Stoping and the mechanisms of emplacement of the granites in the Western Ring Complex of the Galway granite batholith, western Ireland. *Earth and Environmental Science Transactions of the Royal Society of Edinburgh* **102**, 1–16.

Leake, B. E., Tanner, P. W. G., Singh, D. & Halliday, A. N. 1983. Major southward thrusting of the Dalradian rocks of Connemara, western Ireland. *Nature* **305**, 210–13.

Leake, B. E. & Tanner, G. P. W. 1994. *The Geology of the Dalradian and Associated Rocks of Connemara, Western Ireland*. Dublin: Royal Irish Academy. 96 pp.

Leggo, P. J., Compston, W. & Leake, B. E. 1966. The geochronology of the Connemara granites and its bearing on the antiquity of the Dalradian Series. *Quarterly Journal of the Geological Society*, London **122**, 91–116.

Long, C. B. & McConnell, B. 1995. Bedrock Geology, 1:100,000 Series. *Geological Survey of Ireland* **Sheet 10**.

Madden, J. S. 1987. *Gamma-ray spectrometric studies of the main Galway Granite, Connemara, western Ireland*. PhD Thesis, National University of Ireland.

Magee, C., Stevenson, C. T. E., Driscoll, B. O. & Petronis, M. S. 2012. Local and regional controls on the lateral emplacement of the Ben Hiant Dolerite intrusion, Ardnamurchan (NW Scotland). *Journal of Structural Geology* **39**, 66–82.

Max, M. D., Long, C. B. & Geoghegan, M. A. 1978. The Galway Granite. *Bulletin of the Geological Survey of Ireland* **2**, 431–51.

McCarthy, W. 2013. *An evaluation of orogenic kinematic evolution utilizing crystalline and magnetic anisotropy in granitoids*. PhD Thesis, University College Cork, National University of Ireland.

McCarthy, W., Petronis, M. S., Reavy, R. J. & Stevenson, C. T. E. 2015. Distinguishing diapirs from inflated plutons; an integrated rock magnetic, magnetic fabric and structural study on the Roundstone Pluton, western Ireland. *Journal of the Geological Society, London* **172,** 550–65.

Meere, P. A. & Mulchrone, K. F. 2006. Timing of deformation within Old Red Sandstone lithologies from the Dingle Peninsula, SW Ireland. *Journal of the Geological Society*, *London* **163**, 461–69.

Molyneux, S. J. & Hutton, D. H. W. 2000. Evidence for significant granite space creation by the ballooning mechanism: The example of the Ardara pluton, Ireland. *Geological Society of America Bulletin* **112**, 1543–58.

Neilson, J. C., Kokelaar, B. P. & Crowley, Q. G. 2009. Timing, relations and cause of plutonic and volcanic activity of the Siluro-Devonian post-collision magmatic episode in the Grampian Terrane, Scotland. *Journal of the Geological Society*, *London* **166**, 545–61.

Owens, W. H. 1974. Mathematical model studies on factors affecting the magnetic anisotropy of deformed rocks. *Tectonophysics* **24**, 115–31.

Owens, W. H. 2000. Statistical analysis of normalized and unnormalized second rank tensor data, with application to measurements of anisotropy of magnetic susceptibility. *Geophysical Research Letters* **27**, 2985–88.

Parés, J. M. & van der Pluijm, B. A. 2002. Evaluating magnetic lineations (AMS) in deformed rocks. *Tectonophysics* **350**, 283–98.

Passchier, C. W. & Trouw, R. A. J. 2005. *Microtectonics*. Berlin Heidelberg New York: Springer-Verlag. 366 pp.

Pe-Piper, G., Piper, D. J. W. & Matarangas, D. 2002. Regional implications of geochemistry and style of emplacement of Miocene I-type diorite and granite, Delos, Cyclades, Greece. *Lithos* **60**, 47–66.

Petronis, M. S., Hacker, D. B., Holm, D. K., Geissman, J. W. & Harlan, S. S. 2004. Magmatic flow paths and palaeomagnetism of the Miocene Stoddard Mountain laccolith, Iron Axis region, Southwestern Utah, USA. *Geological Society, London, Special Publications* **238**, 251–83.

Petronis, M. S., Driscoll, B. O., Stevenson, C. T. E. & Reavy, R. J. 2012. Controls on emplacement of the Caledonian Ross of Mull Granite, NW Scotland: Anisotropy of magnetic susceptibility and magmatic and regional structures. *Geological Society of America Bulletin* **124**(5/6), 906–27.

Pitcher, W. S. 1998. *The Nature and Origin of Granite*, 2nd edition. London: Chapman & Hall. 387 pp.

Pitcher, W. S. & Bussell, M. A. 1977. Structural control of batholithic emplacement in Peru: a review. *Journal of the Geological Society, London* **133**, 249–55.

Richey, J. E. 1932. Tertiary ring structures in Britain. *Transactions of the Geological Society of Glasgow* **19**, 42–140.

Ryan, P. D., Snyderj, D. B., England, R. W., Soper, N. J., Snyder, D. B. & Hutton, D. H. W. 1995. The Antrim–Galway Line: a resolution of the Highland Border Fault enigma of the Caledonides of Britain and Ireland. *Geological Magazine* **132**, 171–84.

Schofield, N., Heaton, L., Holford, S. P., Archer, S. G., Jackson, C. A. L. & Jolley, D. W. 2012. Seismic imaging of 'broken bridges': linking seismic to outcrop-scale investigations of intrusive magma lobes. *Journal of the Geological Society, London* **169**, 421–26.

Selby, D., Creaser, R. A. & Feely, M. 2004. Accurate and precise Re–Os molybdenite dates from the Galway Granite, Ireland. Critical comment on 'Disturbance of the Re–Os chronometer of molybdenites from the late-Caledonian Galway Granite, Ireland, by hydrothermal fluid circulation'. *Geochemical Journal* **38**, 291–94.

Soper, N. J. & Woodcock, N. H. 2003. The lost Lower Old Red Sandstone of England and Wales: a record of post-Iapetan flexure or Early Devonian transtension? *Geological Magazine* **140**, 627–47.

Stevenson, C. T. E., Hutton, D. H. W. & Price, A. R. 2008. The Trawenagh Bay Granite and a new model for the emplacement of the Donegal Batholith. *Transactions of the Royal Society of Edinburgh: Earth Sciences* **97**(for 1996), 455–77.

Stone, P., Kimbell, G. S. & Henney, P. J. 1997. Basement control on the location of strike-slip shear in the Southern Uplands of Scotland. *Journal of the Geological Society, London* **154**, 141–44.

Suzuki, K., Feely, M. & O'Reilly, C. 2001. Disturbance of the Re–Os chronometer of molybdenites from the late-Caledonian Galway Granite, Ireland, by hydrothermal fluid circulation. *Geochemical Journal* **35**, 29–35.

Tanner, P. W. G., Dempster, T. J. & Dickin, A. P. 1989. Short Paper: Time of docking of the Connemara terrane with the Delaney Dome Formation, western Ireland. *Journal of the Geological Society, London* **146**, 389–92.

Tarling, D. H. & Hrouda, F. (eds) 1993. *The Magnetic Anisotropy of Rocks*. London: Chapman & Hall. 217 pp.

Townend, R. 1966. The geology of some granite plutons from western Connemara, Co. Galway. *Proceedings of the Royal Irish Academy* **65 Section**, 157–202.

Treloar, P. J. 1977. *The stratigraphy, geochemistry and metamorphism of the rocks of the Recess area, Connemara, Eire*. PhD Thesis, University of Glasgow, UK.

Treloar, P. J. 1982. The stratigraphy and structure of the rocks of the Lissoughter area, Connemara. *Proceedings of the Royal Irish Academy* **82 Section**, 83–107.

Valley, P. M., Hanchar, J. M. & Whitehouse, M. J. 2011. New insights on the evolution of the Lyon Mountain Granite and associated Kiruna-type magnetite-apatite deposits, Adirondack Mountains, New York State. *Geosphere* **7**, 357–89.

Vance, A. J. 1969. On Synneusis. *Contributions to Mineralogy and Petrology* **24**, 7–29.

Vernon, R. H. 2004. *A practical guide to Rock Microstructure*. Cambridge, UK: Cambridge University Press. 594 pp.

Woodcock, N. H., Soper, N. J. & Strachan, R. A. 2007. A Rheic cause for the Acadian deformation in Europe. *Journal of the Geological Society, London.* **164** 1023–36.

Wright, P. C. 1964. The petrology, chemistry and structure of the Galway granite of the Carna area, County Galway. *Proceedings of the Royal Irish Academy* **62 Section**, 239–64.

MS received 3 June 2014. Accepted for publication 20 July 2015.